

String fragmentation of a quark pair with entangled spin states: Application to e^+e^- annihilation

A. Kerbizi^{1,*} and X. Artru^{2,†}

¹*Dipartimento di Fisica, Università degli Studi di Trieste and INFN Sezione di Trieste,
Via Valerio 2, 34127 Trieste, Italy*

²*Université de Lyon, Institut de Physique des deux Infinis (IP2I Lyon), Université Lyon 1 and CNRS,
4 rue Enrico Fermi, F-69622 Villeurbanne, France*

 (Received 22 December 2023; accepted 21 February 2024; published 20 March 2024)

We present a recursive quantum mechanical model for the fragmentation of a string stretched between a quark and an antiquark with entangled spin states. The quarks are assumed to be produced in the e^+e^- annihilation process via the exchange of a virtual photon and the correlations between their spin states are described by a joint spin-density matrix. The string fragmentation process is formulated at the amplitude level by using the splitting matrices of the recent string $+^3P_0$ model of polarized quark fragmentation with pseudoscalar and vector meson emissions and accounts for the systematic propagation of the spin correlations in the fragmentation chain. The model is formulated as a recursive recipe suitable for a Monte Carlo implementation. It reproduces the expected angular correlation, due to the Collins effect, between back-to-back pseudoscalar and/or vector mesons. For the latter, this correlation also involves the momenta of the decay products. We use the model for studying the sign of the Collins asymmetry for back-to-back vector and pseudoscalar mesons.

DOI: [10.1103/PhysRevD.109.054029](https://doi.org/10.1103/PhysRevD.109.054029)

I. INTRODUCTION

The e^+e^- annihilation to hadrons is an important process to study the hadronization of quarks and gluons in the observed hadrons, a still poorly understood phenomenon of the strong interactions. According to the factorization theorem in quantum chromodynamics (QCD) [1], the cross section can be factorized in the cross section for the annihilation reaction $e^+e^- \rightarrow q_1\bar{q}_1$ and in the fragmentation functions (FFs) that describe the conversion of the quark q_1 and antiquark \bar{q}_1 in the observed hadrons. Recently the e^+e^- annihilation has been used as a tool to access the class of spin-dependent FFs. Examples are the Collins function $H_{1q}^{\perp h}$ [2], which describes the fragmentation of a transversely polarized quark q_1 in an unpolarized hadron h , and the interference fragmentation function (IFF) $H_{1q}^{\langle hh \rangle}$ [3,4], which describes the fragmentation of a transversely polarized quark q_1 in a pair of unpolarized hadrons hh .

In e^+e^- annihilation cross section, the spin-dependent FFs give birth to azimuthal modulations in the distribution of the observed hadrons. The amplitudes of these modulations are referred to as asymmetries and provide access to the spin-dependent FFs (for a review see, e.g., Ref. [5]). The semi-inclusive annihilation process $e^+e^- \rightarrow h_1h_2X$, where one of the hadrons h_1 or h_2 is assumed to be produced in the quark jet and the other in the antiquark jet, allows one to measure the Collins asymmetry originated from the coupling of two Collins FFs [5]. If two hadrons are observed in each quark jet by the process $e^+e^- \rightarrow (h_1h_2)(\bar{h}_1\bar{h}_2)X$, the Artru-Collins asymmetry [6] appears, which allows one to access the product of two IFFs. The Collins asymmetries have been measured in e^+e^- by the BELLE [7,8], BABAR [9,10] and BESIII [11] experiments, whereas the Artru-Collins asymmetries have been measured by the BELLE experiment [12].

The e^+e^- asymmetry data have played a fundamental role in the investigation of the partonic structure of the nucleons. The data have been analyzed in combination with the data from semi-inclusive deep inelastic scattering (SIDIS) of leptons off transversely polarized nucleons on the Collins asymmetries [2] and on the dihadron production asymmetry [3,4] to extract the spin-dependent FFs and the transversity parton distribution function (see, e.g., Refs. [13–20]). Transversity describes the transverse polarization of quarks in a transversely polarized nucleon and is the third parton distribution function needed to characterize

*albi.kerbizi@ts.infn.it

†x.артру@ipnl.in2p3.fr

Published by the American Physical Society under the terms of the Creative Commons Attribution 4.0 International license. Further distribution of this work must maintain attribution to the author(s) and the published article's title, journal citation, and DOI. Funded by SCOAP³.

the collinear partonic structure of the nucleon at leading order.

This work is dedicated to the modeling of spin effects in e^+e^- annihilation to hadrons with the final goal of implementing the model in a Monte Carlo event generator (MCEG). Recently, the spin effects have been implemented for the simulation of the polarized SIDIS process in the PYTHIA 8 MCEG [21,22] by the *StringSpinner* package [23,24]. The simulation of the spin effects is based on the string $+^3P_0$ model of polarized hadronization [25–27], which is implemented in *StringSpinner*. It is a quantum mechanical extension of the Lund model [28] of string fragmentation that includes the quark spin degree of freedom at the amplitude level. An analog MCEG for e^+e^- annihilation with spin effects presently does not exist, the main difficulty coming from the nonclassical (entangled) correlation of the q_1 and \bar{q}_1 spins.

Up to now, the string $+^3P_0$ model has been applied to the description of the recursive fragmentation of a string, starting from one end drawn by a polarized quark or antiquark without taking care of the polarization of the object (quark or diquark) drawing the opposite end. Thus it cannot be applied as it stands to e^+e^- annihilation where both q_1 and \bar{q}_1 are polarized, which is more in an entangled fashion [29]. Here we extend the string $+^3P_0$ model to the description of the fragmentation of a string stretched between a quark q_1 and an antiquark \bar{q}_1 with entangled spin states. The correlation between their spin states is described by the means of a joint spin-density matrix of the pair. The joint spin-density matrix is calculated assuming the e^+e^- annihilation to be mediated by a virtual photon. The model is however general and it does not depend on the mechanism invoked for the production of the $q_1\bar{q}_1$ pair. The rules of the string $+^3P_0$ model with emission of pseudo-scalar (PS) mesons and vector mesons (VMs) [27] are used to describe the hadron emissions from the quark and antiquark ends of the string. To take into account the quantum mechanical correlations between the two end points of the string after hadron emissions we employ a recipe inspired from the Collins-Knowles (CK) recipe [30–32]. The CK recipe is applied to involve in the correlation not only the momentum of a VM, but also the individual momenta of its decay products. Finally we formulate a recursive recipe for the simulation of the string fragmentation of a $q_1\bar{q}_1$ pair with correlated spin states that is suitable for a Monte Carlo implementation. The recipe is applied to the production of the two leading hadrons in $e^+e^- \rightarrow h_1h_2X$ showing that it reproduces the expected modulations in the azimuthal distribution of the hadrons [5,33].

Throughout the article we neglect gluon emissions from the quark and the antiquark. Such emissions transform the $q_1 - \bar{q}_1$ string into a broken line with corners at the gluons. Besides, the gluons are polarized in correlation with the spins of q_1 and \bar{q}_1 . The present formulation of the string $+^3P_0$ model is insufficient for handling this situation. The

present work is, however, necessary before the generalization of the string $+^3P_0$ model to more general string configurations, which deserves future works.

The article is organized as follows. In Sec. II we give the main ingredients needed for the modeling of the spin effects in e^+e^- annihilation. In Sec. III the different steps needed to describe the fragmentation of a string stretched between a quark pair with entangled spin state are discussed and the final recursive recipe suitable for Monte Carlo implementation is given. The recipe is applied to the production of two back-to-back hadrons in Sec. IV. Finally the conclusions are drawn in Sec. V.

II. PHYSICS INGREDIENTS FOR MODELING SPIN EFFECTS IN e^+e^- ANNIHILATION

Following the factorization theorem [1], we factorize the annihilation process $e^+e^- \rightarrow q_1\bar{q}_1 \rightarrow h_1, h_2, \dots, h_N$, where h_1, h_2, \dots, h_N are the final state hadrons, into a hard subprocess, where the quark pair $q_1\bar{q}_1$ is created in the annihilation $e^+e^- \rightarrow q_1\bar{q}_1$, and a soft process $q_1\bar{q}_1 \rightarrow h_1, h_2, \dots, h_N$, where the quark pair hadronizes into the final state hadrons. The framework for the description of the hard subprocess is set up in Sec. II B from the kinematical point of view and in Appendix A from the dynamical point of view.

We describe the hadronization of the $q_1\bar{q}_1$ pair by an extension of the string $+^3P_0$ model to the fragmentation of a string stretched between q_1 and \bar{q}_1 , which have correlated spin states. To this end in Sec. II A we introduce the folded unitarity diagram (Fig. 1) for the process $e^+e^- \rightarrow q_1\bar{q}_1 \rightarrow hHX$, where h and H are hadrons associated to the q_1 and \bar{q}_1 jets, respectively. The diagram is related to the cross section of the process, which depends on the joint spin-density matrix of the $q_1\bar{q}_1$ pair and on the splitting amplitudes for the recursive emissions of hadrons from the quarks. The joint spin-density matrix of the $q_1\bar{q}_1$ pair is described in Sec. II C, while the splitting amplitudes, which

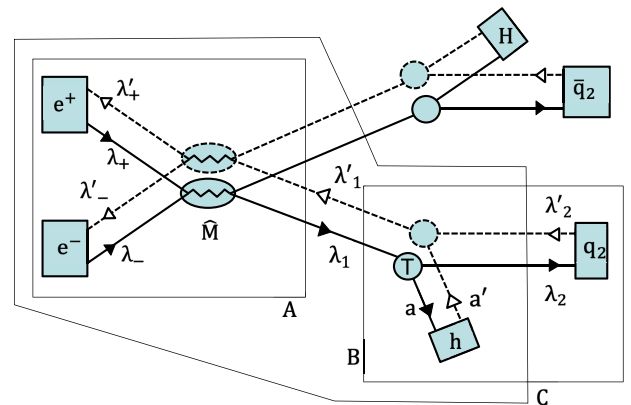


FIG. 1. Folded unitarity diagram for the reaction $e^+e^- \rightarrow q_1\bar{q}_1$ followed by the splittings $q_1 \rightarrow h + X$ and $\bar{q}_1 \rightarrow H + X'$.

are taken from the string $+^3P_0$ model of Ref. [27], are recalled in Sec. II D.

A. The unitarity diagram for e^+e^- annihilation

1. Conventions for the figures

We represent the probability of a reaction by a pair of Feynman-like diagrams, slightly shifted from each other: a direct diagram with black arrow points for the amplitude and a reversed diagram with white arrow points for the complex conjugate amplitude (see, e.g., Fig. 1). This representation is obtained by folding the standard, left-right symmetrical, unitarity diagram. Gray blobs represent subprocess amplitudes. Greek letters label the spin states of fermions, Latin letters those of bosons. These letters are primed for the conjugate amplitude.

Gray rectangles represent sources of initial particles or detectors of final particles. A source is characterized by a density or *emittance*¹ matrix $\langle \lambda | \rho | \lambda' \rangle$ and a detector by an *acceptance matrix* [34] $\langle \lambda' | \eta | \lambda \rangle$. For an unpolarized source (respectively, detector), the $\delta_{\lambda, \lambda'}$ is represented by a U turn $\curvearrowright^{\leftarrow}$ (respectively, $\curvearrowleft^{\rightarrow}$) of the particle line inside the gray rectangle. Also, the unit acceptance matrix is indicated by η^U in the figures.

2. Elements of the unitarity diagram

To introduce the main ingredients required for the description of e^+e^- annihilation, we start by the folded unitarity diagram for the process $e^+e^- \rightarrow q_1\bar{q}_1 \rightarrow hHX$ shown in Fig. 1. The hadron h is emitted in the quark splitting $q_1 \rightarrow h + q_2$. The hadron H is emitted in the antiquark splitting $\bar{q}_1 \rightarrow H + \bar{q}_2$. The fragmentation chains initiated by the leftover quarks q_2 and \bar{q}_2 are not shown explicitly but summarized by acceptance matrices represented by gray boxes.

To the folded unitarity diagram is associated the two-particle inclusive cross section

$$\begin{aligned} d\sigma(e^+\uparrow e^-\uparrow \rightarrow hHX) &\propto \langle \lambda_2 | T_{q_2, h, q_1} | \lambda_1 \rangle \langle \bar{\lambda}_2 | T_{\bar{q}_2, H, \bar{q}_1} | \bar{\lambda}_1 \rangle \\ &\times \langle \lambda_1, \bar{\lambda}_1 | \hat{\mathcal{M}} | \lambda_-, \lambda_+ \rangle \rho_{\lambda_-, \lambda_+}^{e^-} \rho_{\lambda_+, \lambda_+}^{e^+} \langle \lambda'_-, \lambda'_+ | \hat{\mathcal{M}}^\dagger | \lambda'_1, \bar{\lambda}'_1 \rangle \\ &\times \langle \lambda'_1 | T_{q_2, h, q_1}^\dagger | \lambda'_2 \rangle \langle \bar{\lambda}'_1 | T_{\bar{q}_2, H, \bar{q}_1}^\dagger | \bar{\lambda}'_2 \rangle \\ &\times \langle \lambda'_2 | \eta(q_2) | \lambda_2 \rangle \langle \bar{\lambda}'_2 | \eta(\bar{q}_2) | \bar{\lambda}_2 \rangle, \end{aligned} \quad (1)$$

where the repeated indices are summed over. The second line in Eq. (1) expresses the production of the $q_1\bar{q}_1$ pair from the annihilation of the e^+ and e^- . It describes the hard subprocess $e^+e^- \rightarrow q_1\bar{q}_1$. The first and third lines describe the splittings $q_1 \rightarrow h + q_2$ and $\bar{q}_1 \rightarrow H + \bar{q}_2$ in the amplitude and the complex conjugated amplitude,

respectively. The last line expresses possible further information coming from the successive splittings of q_2 and \bar{q}_2 . The meaning of the different components of the amplitude is as follows.

The quantity $\hat{\mathcal{M}}$ indicates the quantum amplitude associated to the hard process $e^+(\lambda_+)e^-(\lambda_-) \rightarrow q_1(\lambda_1)\bar{q}_1(\bar{\lambda}_1)$. We have labeled with λ_+ , λ_- , λ_1 , and $\bar{\lambda}_1$ the helicities of e^+ , e^- , q_1 , and \bar{q}_1 , respectively. The quantum states $|\lambda_-, \lambda_+\rangle$ and $|\lambda_1, \bar{\lambda}_1\rangle$ indicate, respectively, the two-particle helicity states $|\lambda_-\rangle \otimes |\lambda_+\rangle$ and $|\lambda_1\rangle \otimes |\bar{\lambda}_1\rangle$. $\hat{\mathcal{M}}_{\lambda_-, \lambda_+, \lambda_1, \bar{\lambda}_1} \equiv \langle \lambda_1, \bar{\lambda}_1 | \hat{\mathcal{M}} | \lambda_-, \lambda_+ \rangle$ is the helicity amplitude, which can be calculated perturbatively using standard methods. The expressions that we obtain are given for completeness in Appendix A.

The quantities $\rho_{\lambda_-, \lambda_+}^{e^-}$ and $\rho_{\lambda_+, \lambda_+}^{e^+}$, represented by the gray boxes on the left of Fig. 1, are the spin-density matrices of the e^- and e^+ , respectively. They contain the information on the spin states of the beam particles. In the following we assume the electron and positron to be unpolarized, i.e. $\rho_{\lambda_-, \lambda_+}^{e^-} = \delta_{\lambda_-, \lambda_+}/2$ and $\rho_{\lambda_+, \lambda_+}^{e^+} = \delta_{\lambda_+, \lambda_+}/2$.

The operator T_{q_2, h, q_1} , represented by the lowest gray disk in Fig. 1, indicates the quantum amplitude for the splitting of a quark q_1 in a hadron h and a leftover quark q_2 . It will be referred to as the splitting matrix. The matrix elements of the splitting matrix are indicated by $\langle \lambda_2 | T_{q_2, h, q_1} | \lambda_1 \rangle$, where the index λ_2 labels the spin state of the quark q_2 . We have assumed for the moment the hadron h to be spinless ($a = a' = 0$). The same definitions apply to the splitting matrix $T_{\bar{q}_2, H, \bar{q}_1}$ (second upper gray disk in Fig. 1) that describes the splitting of the antiquark \bar{q}_1 in the hadron H and the leftover antiquark \bar{q}_2 . The corresponding matrix elements are $\langle \bar{\lambda}_2 | T_{\bar{q}_2, H, \bar{q}_1} | \bar{\lambda}_1 \rangle$, where $\bar{\lambda}_2$ labels the spin state of \bar{q}_2 . The hadron H is also taken to be spinless, for the moment. The splitting matrices for the quark and antiquark, taken from the string $+^3P_0$ model in Ref. [27], are described in detail in Sec. II D.

The quantity $\eta(q_2)$ is the *acceptance matrix* of q_2 . If quarks were not confined, it could characterize a polarized detector for q_2 . In reality it carries the spin information coming ‘‘backward in time’’ from the analysis of particles further produced in the fragmentation chain (for the definition and the use of the acceptance matrices see Ref. [34]). The associated matrix elements are $\langle \lambda'_2 | \eta(q_2) | \lambda_2 \rangle$. If there is no information coming from the future emissions of q_2 , or equivalently if that information is integrated over, the acceptance matrix is the identity matrix $\langle \lambda'_2 | \eta(q_2) | \lambda_2 \rangle = \delta_{\lambda'_2, \lambda_2}$. The acceptance matrix $\eta(\bar{q}_2)$ for the antiquark \bar{q}_2 has a similar meaning. More rigorously, the acceptance matrices $\eta(q_2)$ and $\eta(\bar{q}_2)$ should be gathered in one 4×4 matrix $\eta(q_2, \bar{q}_2)$, which takes into account the spin correlations transmitted by closing the quark line. In this model we neglect such correlations and decompose $\eta(q_2, \bar{q}_2) = \eta(q_2) \otimes \eta(\bar{q}_2)$.

¹If not normalized to unit trace.

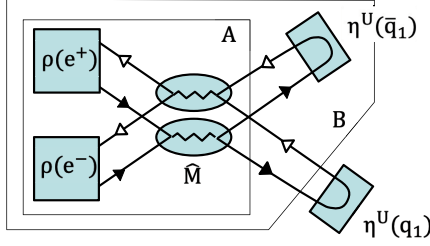


FIG. 2. Folded unitarity diagram for the reaction $e^+e^- \rightarrow q_1\bar{q}_1$. η^U is the unit 2×2 acceptance matrix. Rectangle A: $\langle |\hat{\mathcal{M}}|^2 \rangle \rho(q_1, \bar{q}_1)$. Domain B: $\langle |\hat{\mathcal{M}}|^2 \rangle \rho(q_1)$ [Eq. (5a)].

The cross section in Eq. (1) can be further simplified to obtain the expression

$$\begin{aligned} d\sigma(e^+e^- \rightarrow hHX) & \propto \langle \lambda_1, \bar{\lambda}_1 | \hat{\mathcal{M}} | \lambda_-, \lambda_+ \rangle \rho_{\lambda_-, \lambda_+}^{e^-} \rho_{\lambda_+, \lambda_-}^{e^+} \\ & \times \langle \lambda'_-, \lambda'_+ | \hat{\mathcal{M}}^\dagger | \lambda'_1, \bar{\lambda}'_1 \rangle \times \langle \lambda'_1 | \eta(q_1) | \lambda_1 \rangle \langle \bar{\lambda}'_1 | \eta(\bar{q}_1) | \bar{\lambda}_1 \rangle \\ & \equiv |\hat{\mathcal{M}}|^2 \text{Tr}_{q_1\bar{q}_1} [\rho(q_1, \bar{q}_1) \eta(q_1) \otimes \eta(\bar{q}_1)]. \end{aligned} \quad (2)$$

The different pieces of the cross section are gathered to define the spin-summed squared amplitude $|\hat{\mathcal{M}}|^2$ associated to the hard subprocess, the joint spin-density matrix $\rho(q_1, \bar{q}_1)$ of the $q_1\bar{q}_1$ pair (represented in Fig. 1 by the rectangular domain A), and the acceptance matrices $\eta(q_1)$ for the initial quark q_1 and $\eta(\bar{q}_1)$ for the initial antiquark \bar{q}_1 . The operation $\text{Tr}_{q_1\bar{q}_1}$ indicates the trace over the spin indices of q_1 and \bar{q}_1 .

The squared amplitude $|\hat{\mathcal{M}}|^2$ is related to the cross section of the hard scattering $e^+e^- \rightarrow q_1\bar{q}_1$ for not-analyzed quarks, and it is given by

$$|\hat{\mathcal{M}}|^2 \equiv \langle \lambda_1, \bar{\lambda}_1 | \hat{\mathcal{M}} | \lambda_-, \lambda_+ \rangle \rho_{\lambda_-, \lambda_+}^{e^-} \rho_{\lambda_+, \lambda_-}^{e^+} \langle \lambda'_-, \lambda'_+ | \hat{\mathcal{M}}^\dagger | \lambda_1, \bar{\lambda}_1 \rangle. \quad (3)$$

It is represented by the folded unitarity diagram in Fig. 2.

Concerning the acceptance matrices $\eta(q_1)$ and $\eta(\bar{q}_1)$, they can be obtained by comparing Eq. (2) with Eq. (1). The expressions are

$$\begin{aligned} \langle \lambda'_1 | \eta(q_1) | \lambda_1 \rangle & = \langle \lambda'_1 | T_{q_2, h, q_1}^\dagger | \lambda'_2 \rangle \langle \lambda'_2 | \eta(q_2) | \lambda_1 \rangle \langle \lambda_1 | T_{q_2, h, q_1} | \lambda_1 \rangle, \\ \langle \bar{\lambda}'_1 | \eta(\bar{q}_1) | \bar{\lambda}_1 \rangle & = \langle \bar{\lambda}'_1 | T_{\bar{q}_2, H, \bar{q}_1}^\dagger | \bar{\lambda}'_2 \rangle \langle \bar{\lambda}'_2 | \eta(\bar{q}_2) | \bar{\lambda}_1 \rangle \langle \bar{\lambda}_1 | T_{\bar{q}_2, H, \bar{q}_1} | \bar{\lambda}_1 \rangle, \end{aligned} \quad (4a)$$

and, when written in matrix form, they are

$$\begin{aligned} \eta(q_1) & = T_{q_2, h, q_1}^\dagger \eta(q_2) T_{q_2, h, q_1}, \\ \eta(\bar{q}_1) & = T_{\bar{q}_2, H, \bar{q}_1}^\dagger \eta(\bar{q}_2) T_{\bar{q}_2, H, \bar{q}_1}. \end{aligned} \quad (4b)$$

These matrices bring to the hard scattering the spin information from the splittings of q_1 and \bar{q}_1 . The diagrammatic

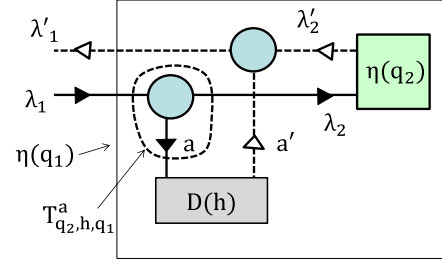


FIG. 3. Derivation of the acceptance matrix $\eta(q_1)$ from $\eta(q_2)$ and $\eta(h) \equiv D(h)$. It applies to Eqs. (4a) and (4b), taking $\eta(h) = 1$.

representation of $\eta(q_1)$ is shown in Fig. 3 for h of arbitrary spin. For the spinless case, $a = a' = 0$, $\eta(h) = 1$. $\eta(q_1)$ is also indicated in Fig. 1 by the rectangular domain B. A similar diagram can be drawn for $\eta(\bar{q}_1)$.

From Eq. (2) one can obtain the cross section for single hadron production $e^+e^- \rightarrow hX$ by taking $\eta(\bar{q}_1) = 1^{\bar{q}_1}$. It is

$$d\sigma(e^+e^- \rightarrow hX) \propto |\hat{\mathcal{M}}|^2 \text{Tr}[\rho(q_1) \eta(q_1)], \quad (5a)$$

where

$$\rho(q_1) = \text{Tr}_{\bar{q}_1} \rho(q_1, \bar{q}_1) \quad (5b)$$

is the spin-density matrix of q_1 obtained by the partial trace over the spin indices of \bar{q}_1 . It is represented in Fig. 2 by the domain B. The cross section in Eq. (5a) is represented by the full diagram of Fig. 2 but removing the U-turn in the lower-right gray rectangle and the upper index U for $\eta(q_1)$. It is well known that the single hadron production in e^+e^- cannot be used for studying transverse spin effects due to the fact that the quark (and the antiquark) is unpolarized, as can be seen from Eqs. (5b) and (11).

Independently of $\rho(q_1)$, the reaction in Eq. (5a) has been used for the study of the spin alignment of VMs in hadronic Z^0 decays [35–37] and recently has gained interest in the context of the phenomenology of the transverse-momentum-dependent spin-averaged FFs [38].

B. The hard scattering

The kinematics of the hard scattering $e^+(p_+)e^-(p_-) \rightarrow q_1(k_1)\bar{q}_1(\bar{k}_1)$, where in the parentheses we have indicated the four-momentum of each particle, is shown in Fig. 4 in the center of mass system (c.m.s.). As already mentioned in the introduction, we neglect the gluon radiation from the quarks. The four-momenta are given by

$$\begin{aligned} p_\mp & = \frac{\sqrt{s}}{2} (1, \mp \sin \theta, 0, \pm \cos \theta), \\ k_1 & = \frac{\sqrt{s}}{2} (1, 0, 0, \beta_q), \quad \bar{k}_1 = \frac{\sqrt{s}}{2} (1, 0, 0, -\beta_q). \end{aligned} \quad (6)$$

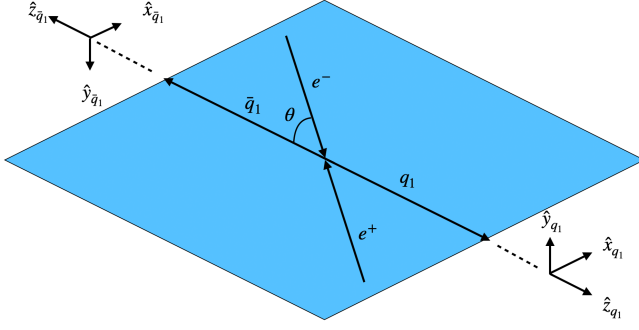


FIG. 4. Kinematics of the annihilation process $e^+e^- \rightarrow q_1\bar{q}_1$ in the c.m.s. Also shown are the axes of the helicity frames of the quark and the antiquark.

The electron mass is neglected as it is much smaller than the considered values of the center of mass energy $\sqrt{s} = \sqrt{2p_+ \cdot p_-}$. θ is the angle between the \mathbf{p}_- and \mathbf{k}_1 . The quantity $\beta_q = \sqrt{1 - 4m_q^2/s}$ is the velocity of the quark and m_q is the quark mass.²

The hard scattering differential cross section is related to the squared matrix element in Eq. (3) by $d\hat{\sigma}/d\cos\theta = 3\beta_q |\hat{\mathcal{M}}|^2 / (32\pi s)$, where the factor 3 is included to account for the number of quark colors. Using the expressions for the helicity amplitudes in Appendix A, we obtain the known angular distribution [39]

$$\frac{d\hat{\sigma}(q_1\bar{q}_1)}{d\cos\theta} = \frac{3\pi\alpha^2}{2s} e_q^2 \beta_q [1 + \cos^2\theta + (1 - \beta_q)^2 \sin^2\theta]. \quad (7)$$

In the c.m.s., we introduce the so-called helicity frames of the quark and the antiquark. They are the reference systems attached to the quark and the antiquark that are introduced when calculating the helicity amplitudes in Appendix A.³ We represent the quark helicity frame (QHF) with the set of axes $\{\hat{\mathbf{x}}_{q_1}, \hat{\mathbf{y}}_{q_1}, \hat{\mathbf{z}}_{q_1}\}$ and the antiquark helicity frame (AHF) with the set of axes $\{\hat{\mathbf{x}}_{\bar{q}_1}, \hat{\mathbf{y}}_{\bar{q}_1}, \hat{\mathbf{z}}_{\bar{q}_1}\}$. The axes are defined to be

$$\begin{aligned} \hat{\mathbf{z}}_{q_1} &= \frac{\mathbf{k}_1}{|\mathbf{k}_1|}, & \hat{\mathbf{y}}_{q_1} &= \frac{\mathbf{p}_- \times \hat{\mathbf{z}}_{q_1}}{|\mathbf{p}_- \times \hat{\mathbf{z}}_{q_1}|}, & \hat{\mathbf{x}}_{q_1} &= \hat{\mathbf{y}}_{q_1} \times \hat{\mathbf{z}}_{q_1}, \\ \hat{\mathbf{z}}_{\bar{q}_1} &= \frac{\bar{\mathbf{k}}_1}{|\bar{\mathbf{k}}_1|}, & \hat{\mathbf{y}}_{\bar{q}_1} &= \frac{\mathbf{p}_- \times \hat{\mathbf{z}}_{\bar{q}_1}}{|\mathbf{p}_- \times \hat{\mathbf{z}}_{\bar{q}_1}|}, & \hat{\mathbf{x}}_{\bar{q}_1} &= \hat{\mathbf{y}}_{\bar{q}_1} \times \hat{\mathbf{z}}_{\bar{q}_1}. \end{aligned} \quad (8)$$

The helicity frames of the quark and the antiquark are shown in Fig. 4. The two frames share their x axes, whereas

²The quark mass is not neglected to account for the mass of charm quarks that is not negligible when compared to the center of mass energy of the BESIII experiment. Taking the mass of the charm quark to be $m_c \simeq 1.5 \text{ GeV}/c^2$, the velocity of charm quarks in the c.m.s. at the BESIII energy is expected to be $\beta_q \simeq 0.55$.

³The definition of the helicity frame can be found, e.g., in Ref. [40]. See also Ref. [33].

the other axes are the opposite. The four-momenta given in Eq. (6) are expressed in the QHF.

Considering a generic vector \mathbf{v} with azimuthal angle $\phi^{(\text{QHF})}(\mathbf{v})$ and polar angle $\theta^{(\text{QHF})}(\mathbf{v})$ measured in the QHF, and azimuthal angle $\phi^{(\text{AHF})}(\mathbf{v})$ and polar angle $\theta^{(\text{AHF})}(\mathbf{v})$ measured in the AHF, the relations among the angles expressed in the two frames are

$$\begin{aligned} \phi^{(\text{AHF})}(\mathbf{v}) &= 2\pi - \phi^{(\text{QHF})}(\mathbf{v}), \\ \theta^{(\text{AHF})}(\mathbf{v}) &= \pi - \theta^{(\text{QHF})}(\mathbf{v}). \end{aligned} \quad (9)$$

These relations are useful to express observables in the same reference system and will be used in Sec. IV.

C. The joint spin-density matrix of the $q_1\bar{q}_1$ pair

In the annihilation $e^+e^- \rightarrow \gamma^* \rightarrow q_1\bar{q}_1$, the virtual photon has spin one and has a nonzero tensor polarization. In addition to a specific θ dependence, this induces correlations among the spin states of q_1 and \bar{q}_1 , which can be encoded in the joint spin-density matrix $\rho(q_1, \bar{q}_1)$ of the $q_1\bar{q}_1$ system.

The expression for the density matrix $\rho(q_1, \bar{q}_1)$ can be obtained from Eq. (2), and it is

$$\begin{aligned} \rho(q_1, \bar{q}_1) &= (|\hat{\mathcal{M}}|^2)^{-1} \hat{\mathcal{M}}_{\lambda_-\lambda_+;\lambda_1\bar{\lambda}_1} \rho_{\lambda_-\lambda_-}^{e^-} \rho_{\lambda_+\lambda_+}^{e^+} \hat{\mathcal{M}}_{\lambda_-\lambda_+;\lambda_1\bar{\lambda}_1}^* \\ &\quad \times |\lambda_1', \bar{\lambda}_1'\rangle \langle \lambda_1, \bar{\lambda}_1| \\ &\equiv \frac{1}{4} C_{\alpha\beta}^{q_1\bar{q}_1} \sigma_\alpha^{q_1} \otimes \sigma_\beta^{\bar{q}_1}. \end{aligned} \quad (10)$$

In the second equality the density matrix is decomposed along a basis spanned by the tensor product of the Pauli matrices $\sigma_\alpha^{q_1} = (1^{q_1}, \sigma_x^{q_1}, \sigma_y^{q_1}, \sigma_z^{q_1})$ for the quark and $\sigma_\beta^{\bar{q}_1} = (1^{\bar{q}_1}, \sigma_x^{\bar{q}_1}, \sigma_y^{\bar{q}_1}, \sigma_z^{\bar{q}_1})$ for the antiquark. The indices α and β take the values 0, x , y , and z . The matrix 1^{q_1} ($1^{\bar{q}_1}$) indicates the identity matrix in the spin space of q_1 (\bar{q}_1). The superscript q_1 (\bar{q}_1) indicates the projection of the vector of Pauli matrices $\boldsymbol{\sigma} = (\sigma^x, \sigma^y, \sigma^z)$ along the axes of the QHF (AHF). The coefficients $C_{\alpha\beta}^{q_1\bar{q}_1}$ introduced in the third line in Eq. (10) express the correlations between the spin states of q_1 and \bar{q}_1 and will be referred to as the correlation coefficients. They can be obtained by taking the trace of Eq. (10) with $\sigma_\alpha^{q_1} \otimes \sigma_\beta^{\bar{q}_1}$. The joint spin-density matrix is normalized such that $C_{00}^{q_1\bar{q}_1} = 1$, and the factor $1/4$ assures that $\text{Tr}_{q_1, \bar{q}_1} \rho(q_1, \bar{q}_1) = 1$.

The nonvanishing correlation coefficients can be calculated using the first line in Eq. (10) and the helicity amplitudes in Table I (see Appendix A). We obtain for the decomposed density matrix

TABLE I. The calculated expressions for $(4\pi\alpha/s)^{-1}\hat{\mathcal{M}}_{\lambda_-, \lambda_+, \lambda_1, \bar{\lambda}_1}$ for the allowed combinations of helicities when taking into account the quark mass and neglecting the electron mass.

Results for $(4\pi\alpha)^{-1}\hat{\mathcal{M}}_{\lambda_-, \lambda_+, \lambda_1, \bar{\lambda}_1}$				
$(\lambda_1, \bar{\lambda}_1)$	(λ_-, λ_+)			
	++	+-	-+	--
+-	$\sin\theta/\gamma_q$	$-(1+\cos\theta)$	$-(1-\cos\theta)$	$\sin\theta/\gamma_q$
+-	$-\sin\theta/\gamma_q$	$-(1-\cos\theta)$	$-(1+\cos\theta)$	$-\sin\theta/\gamma_q$

$$\rho(q_1, \bar{q}_1) = \frac{1}{4} \left[1^{q_1} \otimes 1^{\bar{q}_1} - \frac{2 - (2 - \beta_q^2) \sin^2 \theta}{2 - \beta_q^2 \sin^2 \theta} \sigma_z^{q_1} \otimes \sigma_z^{\bar{q}_1} + \frac{(2 - \beta_q^2) \sin^2 \theta}{2 - \beta_q^2 \sin^2 \theta} \sigma_x^{q_1} \otimes \sigma_x^{\bar{q}_1} + \frac{\beta_q^2 \sin^2 \theta}{2 - \beta_q^2 \sin^2 \theta} \sigma_y^{q_1} \otimes \sigma_y^{\bar{q}_1} + \frac{(1 - \beta_q^2)^{1/2} \sin 2\theta}{2 - \beta_q^2 \sin^2 \theta} (\sigma_x^{q_1} \otimes \sigma_z^{\bar{q}_1} - \sigma_z^{q_1} \otimes \sigma_x^{\bar{q}_1}) \right]. \quad (11)$$

This expression takes into account the nonvanishing quark mass through the dependence on the quark velocity β_q . If the terms depending on the quark mass are neglected, the expression in Eq. (11) is the same as in Ref. [29] when only the terms arising from the exchange of the γ^* are considered.

The joint density matrix in Eq. (11) is not separable, meaning that it cannot be expressed as $\rho(q_1, \bar{q}_1) = \sum_i w_i \rho_i(q_1) \otimes \rho_i(\bar{q}_1)$ with positive weights w_i and density matrices $\rho_i(q_1)$ for the quark and $\rho_i(\bar{q}_1)$ for the antiquark. This is the general case that holds also for other processes, e.g., the Z^0 boson decay $Z^0 \rightarrow q_1 \bar{q}_1$ or the Higgs boson decay $H^0 \rightarrow q_1 \bar{q}_1$. The case of a separable density matrix, e.g., as in the decay $W^\pm \rightarrow q_1 \bar{q}_1$ in the massless quark limit owing to the fact that the W^\pm bosons couple left-handed particles, can be considered as one exception.

D. The splitting matrix of the string + 3P_0 model

We describe the hadronization $q_1 \bar{q}_1 \rightarrow h_1, h_2, \dots, h_N$ in the string fragmentation framework by using the string + 3P_0 model in Ref. [27]. The spacetime picture of the hadronization of the $q_1 \bar{q}_1$ pair in the c.m.s. is depicted in Fig. 5. After being produced at the spacetime point

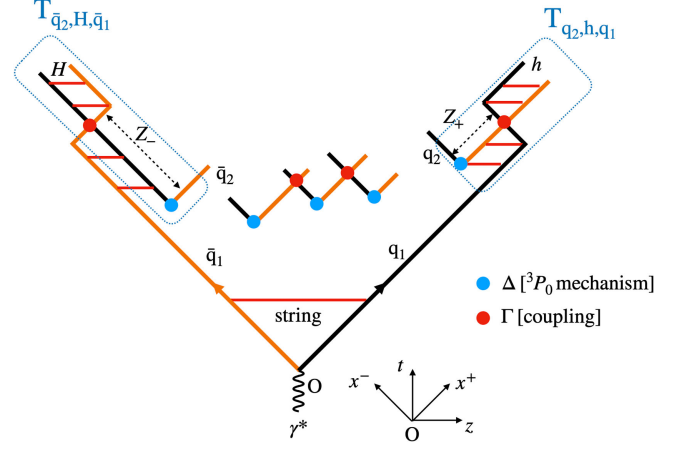


FIG. 5. Spacetime picture of the string fragmentation of the $q_1 \bar{q}_1$ pair. Also shown are the spacetime points where the string breaks via a quark-antiquark pair in the relative 3P_0 state and where quarks couple to the hadrons.

indicated by O , the quark and the antiquark propagate in opposite directions stretching a straight string between them. The string axis is the quark-antiquark axis in the c.m.s., and we take the \hat{z} axis along the quark momentum. In the string fragmentation model, the hadronization can be viewed as the iteration of the elementary quark splitting $q_1 \rightarrow h + q_2$ (top right part of Fig. 5), where the emitted hadron $h = (q_1 \bar{q}_2)$ can be either a PS meson or a VM (baryons and heavier hadronic states are not yet included in the string + 3P_0 model). The leftover quark q_2 propagates the spin information to the next splitting $q_2 \rightarrow h' + q_3$, etc. We indicate the four-momenta of q_1 , h and q_2 by k_1 , p and k_2 , respectively. Momentum conservation implies $p = k_1 - k_2$.

The four-momentum of h is parametrized by introducing the longitudinal splitting variable $Z_+ = p^+/k_1^+$, the transverse momentum \mathbf{p}_T and the transverse energy $\varepsilon_h^2 = \sqrt{M^2 + \mathbf{p}_T^2}$, M being the hadron mass. The light-cone components for a generic four-vector v are defined as $v^\pm = v^0 \pm v^z$. The transverse momentum is $\mathbf{p}_T = (p^x, p^y)$ and we have $\mathbf{p}_T = \mathbf{k}_{1T} - \mathbf{k}_{2T}$.

The model describes the elementary splitting in momentum and spin space by the means of the splitting matrix [27]

$$T_{q_2, h, q_1}(M^2, Z_+, \mathbf{p}_T; \mathbf{k}_{1T}) = C_{q_2, h, q_1} D_h(M^2) \left(\frac{1 - Z_+}{\varepsilon_h^2} \right)^{a/2} e^{-b_L \varepsilon_h^2 / (2Z_+)} N_a^{-1/2} (\varepsilon_h^2) f_T(\mathbf{k}_{2T}^2) \Delta(\mathbf{k}_{2T}) \Gamma_{h, s_h} \hat{u}_{q_1}^{-1/2}(\mathbf{k}_{1T}). \quad (12)$$

The coefficient C_{q_2, h, q_1} describes the splitting in flavor space and it is based on the wave function of h in isospin space. The function $|D_h(M^2)|^2$ gives the invariant mass distribution of h . For a fixed meson mass it is a delta function centered on the nominal squared mass m_h^2 , while

for a resonance it is a relativistic Breit-Wigner function with mass and width fixed to their nominal values (more details can be found in Ref. [27]). The factors involving the Z_+ variable describe the distribution of the longitudinal momentum of h , which depends on the free parameter b_L .

The function $N_a(\varepsilon_h^2)$ depends on the squared transverse energy of h and plays the role of a normalization factor for the Z_+ -dependent part of the splitting amplitude squared. It is given by $N_a^{-1}(\varepsilon_h^2) = \int_0^1 dZ_+ Z_+^{-1} [(1 - Z_+)/\varepsilon_h^2]^a \times \exp(-b_L \varepsilon_h^2/Z_+)$. The function f_T provides the transverse momentum cutoff for the quarks created at string breaking and it is taken to have the exponential form $f_T(\mathbf{k}_{2T}^2) = \exp(-b_T \mathbf{k}_{2T}^2/2)$, with b_T being a free parameter.

The last three terms of Eq. (12) express the spin dependence of the splitting amplitude. The matrix $\Delta(\mathbf{k}_{2T}) = \mu + i\boldsymbol{\sigma} \cdot (\hat{\mathbf{z}}_{q_1} \times \mathbf{k}_{2T}) = \mu + i\sigma_z^{q_1} \boldsymbol{\sigma} \cdot \mathbf{k}_{2T}$ parametrizes the 3P_0 wave function of the $q_2 \bar{q}_2$ pair produced at the string breaking (see Fig. 5) and it depends on the complex mass μ . The latter can in principle depend on the flavor of q_2 and on \mathbf{k}_{2T}^2 , but it is taken to be flavor and \mathbf{k}_{2T}^2 independent. The imaginary part $\text{Im}(\mu)$ is responsible for transverse spin effects, e.g. the Collins effect and the dihadron production asymmetry, while $\text{Im}(\mu^2) = 2\text{Re}(\mu)\text{Im}(\mu)$ is responsible for longitudinal spin effects, e.g., the jet-handedness [25]. The matrix $\boldsymbol{\sigma}_T = (\sigma_x, \sigma_y)$ is the vector of Pauli matrices with only transverse components.

The matrix Γ_{h,s_h} projects the spin state of the $q_1 \bar{q}_2$ pair onto the spin state of the hadron h (see Fig. 5), and it is referred to as the coupling matrix. It is given by

$$\Gamma_{h,s_h} = \begin{cases} \sigma_z & \text{if } h = \text{PS}, \\ G_L 1V_L^* + G_T \boldsymbol{\sigma}_T \sigma_z \cdot \mathbf{V}_T^* & \text{if } h = \text{VM}, \end{cases} \quad (13)$$

where $\mathbf{V} = (V_T, V_L)$ is the linear polarization vector of the VM. In the case of VM emission, the coupling matrix depends on the complex coupling constants G_L and G_T , which describe the coupling of q_1 and q_2 with a VM having longitudinal and transverse polarization with respect to the string axis, respectively. Only the combinations $f_{\text{VM}} = 2|G_T|^2 + |G_L|^2$, $f_L = |G_L|^2/(2|G_T|^2 + |G_L|^2)$

and $\theta_{\text{LT}} = \arg(G_L/G_T)$ are, however, relevant. The parameter f_{VM} gives the ratio between the probability of producing a VM and the probability of producing a PS meson in the elementary splitting. The parameters f_L and θ_{LT} govern the fraction of longitudinally polarized VMs in each splitting and their oblique polarization, respectively.

In the present model, due to the particular choice for $N_a(\varepsilon_h^2)$ [26], the function $\hat{u}_{q_1}(\mathbf{k}_{1T})$ does not depend neither on \mathbf{k}_{1T} nor on the polarization state of q_1 [27]. The latter can be decomposed as

$$\hat{u}_{q_1} = \sum_h \hat{u}_{q_1,h},$$

$$\hat{u}_{q_1,h} = |C_{q_2,h,q_1}|^2 (|\mu|^2 + \langle \mathbf{k}_T^2 \rangle_{f_T}) \begin{cases} 1 & \text{if } h = \text{PS}, \\ f_{\text{VM}} & \text{if } h = \text{VM}, \end{cases} \quad (14)$$

where we have defined $\langle \mathbf{k}_T^2 \rangle_{f_T} = \int d^2 \mathbf{k}_T k_T^2 f_T^2(\mathbf{k}_T^2) / \int d^2 \mathbf{k}_T f_T^2(\mathbf{k}_T^2)$. The ratio $\hat{u}_{q_1,h}/\hat{u}_{q_1}$ gives the relative probability of producing the hadron species h in the elementary splitting.

Due to the left-right (LR) symmetry [28] the string fragmentation process can be viewed equivalently as the iteration of the elementary splitting $\bar{q}_1 \rightarrow H + \bar{q}_2$ of the antiquark \bar{q}_1 in the emitted hadron $H = (\bar{q}_1 q_2)$ and the leftover antiquark \bar{q}_2 (top left part of Fig. 5). To describe the elementary splitting of an antiquark we indicate by \bar{k}_1 and \bar{k}_2 the four-momenta of \bar{q}_1 and \bar{q}_2 and by P the four-momentum of H . The transverse momenta of \bar{q}_1 , H and \bar{q}_2 are indicated by $\bar{\mathbf{k}}_{1T}$, \mathbf{P}_T and $\bar{\mathbf{k}}_{2T}$, respectively. Momentum conservation in the splitting implies $\mathbf{P}_T = \bar{\mathbf{k}}_{1T} - \bar{\mathbf{k}}_{2T}$.

The splitting matrix for the antiquark splitting was not given in Ref. [27]. It can however be obtained from Eq. (12) using the LR symmetry, and it is

$$T_{\bar{q}_2,H,\bar{q}_1}(M^2, Z_-, \mathbf{P}_T; \bar{\mathbf{k}}_{1T}) = C_{\bar{q}_2,H,\bar{q}_1} D_H(M^2) \left(\frac{1 - Z_-}{\varepsilon_H^2} \right)^{a/2} e^{-b_L \varepsilon_H^2/(2Z_-)} N_a^{-1/2}(\varepsilon_H^2) f_T(\bar{\mathbf{k}}_{2T}^2) \Delta(\bar{\mathbf{k}}_{2T}) \Gamma_{H,s_H} \hat{u}_{\bar{q}_1}^{-1/2}(\bar{\mathbf{k}}_{1T}), \quad (15)$$

where it is $\Delta(\bar{\mathbf{k}}_{2T}) = \mu + i\boldsymbol{\sigma} \cdot (\hat{\mathbf{z}}_{\bar{q}_1} \times \bar{\mathbf{k}}_{2T}) = \mu + i\sigma_z^{\bar{q}_1} \boldsymbol{\sigma} \cdot \bar{\mathbf{k}}_{2T}$. It is the same expression as Eq. (12) with the substitutions $q_1 \rightarrow \bar{q}_1$, $h \rightarrow H$, $q_2 \rightarrow \bar{q}_2$ and $Z_+ \rightarrow Z_-$, and $\{\mathbf{k}_{1T}, \mathbf{p}_T, \mathbf{k}_{2T}\} \rightarrow \{\bar{\mathbf{k}}_{1T}, \mathbf{P}_T, \bar{\mathbf{k}}_{2T}\}$. The variable Z_- is defined as $Z_- = P^-/\bar{k}_1^-$ (see Fig. 5).

III. THE POLARIZED FRAGMENTATION OF A STRING WITH ENTANGLED QUARKS

The string + 3P_0 model has been applied to the fragmentation of a string stretched between a quark q_1 on the one end point and an antiquark \bar{q}_1 (or a diquark) on the other end

point, where only the quark polarization is considered [25–27]. The fragmentation chain is thus developed from the quark toward the other end point, and the spin information is propagated only from the quark side.

In this section we extend the string + 3P_0 model of Ref. [27] to the fragmentation of a string stretched between q_1 and \bar{q}_1 with correlated spin states as described by the joint spin-density matrix $\rho(q_1, \bar{q}_1)$. This development is needed for the Monte Carlo simulation of e^+e^- annihilation to hadrons including the quark spin effects. The final recursive recipe for the simulation of e^+e^- annihilation is given in Sec. III B.

A. The steps of the fragmentation chain

1. Hadron emission from the quark end

Pseudoscalar meson emission. We start by considering the emission of a PS meson h from the quark end of the string, i.e. by the splitting $q_1 \rightarrow h + q_2$. The emission of h is described by the probability distribution of emitting the hadron with a given four-momentum. This is obtained neglecting the information coming from the \bar{q}_1 end. Inserting in Eq. (2) the expression of $\eta(q_1)$ given in Eq. (4a) and imposing $\eta(\bar{q}_1) = 1^{\bar{q}_1}$ and $\eta(q_2) = 1^{q_2}$,⁴ we obtain the probability distribution

$$\begin{aligned} & \frac{dP(q_1 \rightarrow h = \text{PS} + q_2; q_1 \bar{q}_1)}{dZ_+ Z_+^{-1} d^2 \mathbf{p}_T} \\ & \equiv F_{q_2, h, q_1}(Z_+, \mathbf{p}_T; \mathbf{k}_{1T}, \mathcal{C}^{q_1 \bar{q}_1}) \\ & = \text{Tr}_{q_2 \bar{q}_1} [\mathbf{T}_{q_2, h, q_1} \rho(q_1, \bar{q}_1) \mathbf{T}_{q_2, h, q_1}^\dagger], \end{aligned} \quad (16)$$

where we have defined $\mathbf{T}_{q_2, h, q_1} = T_{q_2, h, q_1} \otimes 1^{\bar{q}_1}$. The probability distribution is thus obtained by acting with the splitting matrix T_{q_2, h, q_1} on the quark spin subspace of the joint spin-density matrix, with the identity matrix $1^{\bar{q}_1}$ on the antiquark spin subspace (there is yet no information about the emissions from the \bar{q}_1 end) and by taking the trace over the quark and antiquark spin indices. This is represented by the diagram in Fig. 6, ignoring here the buckle to $D^U(h)$. The differential probability $dP(q_1 \rightarrow h = \text{PS} + q_2)$ in the first line in Eq. (16) is divided by the phase space element $dZ_+ Z_+^{-1} d^2 \mathbf{p}_T$.

The function $F_{q_2, h, q_1}(Z_+, \mathbf{p}_T; \mathbf{k}_{1T}, \mathcal{C}^{q_1 \bar{q}_1})$ will be referred to as the splitting function. It describes the energy-momentum sharing between h and q_2 ; it depends on the splitting variable Z_+ and on the transverse momentum \mathbf{p}_T , given the value of the transverse momentum \mathbf{k}_{1T} of q_1 and the values of the correlation coefficients $\mathcal{C}^{q_1 \bar{q}_1}$ that implement the spin correlations between the two string end points. The explicit expression of the splitting function for PS meson emission is obtained inserting in Eq. (16) the Eqs. (12)–(14). The result is (here it depends on $\mathbf{k}_{1T} = \mathbf{0}$, but for iterations of the splitting we will have $\mathbf{k}_{nT} \neq \mathbf{0}$)

$$\begin{aligned} & F_{q_2, h = \text{PS}, q_1}(Z_+, \mathbf{p}_T; \mathbf{k}_{1T}, \mathcal{C}^{q_1 \bar{q}_1}) \\ & = \frac{\hat{u}_{q_1, h}}{\hat{u}_{q_1}} \left(\frac{1 - Z_+}{\epsilon_h^2} \right)^a e^{-b_L \epsilon_h^2 / Z_+} N_a^{-1} (\epsilon_h^2) f_T^2(\mathbf{k}_{2T}^2) \frac{|\mu|^2 + \mathbf{k}_{2T}^2}{|\mu|^2 + \langle \mathbf{k}_T^2 \rangle_T} \\ & \quad \times (1 + \hat{a}(\mathbf{k}_{2T}) \mathcal{C}_{x0}^{q_1 \bar{q}_1} \sin \phi_{\mathbf{k}_2}^{q_1} - \hat{a}(\mathbf{k}_{2T}) \mathcal{C}_{y0}^{q_1 \bar{q}_1} \cos \phi_{\mathbf{k}_2}^{q_1}). \end{aligned} \quad (17)$$

⁴This assumption bears on the fact that, for large enough invariant mass of the remaining $q_2 \bar{q}_1$ system, the spin information decays along the quark fragmentation chain of this system [see Eqs. (31) and (32) of Ref. [26]].

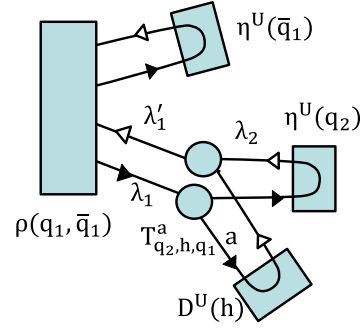


FIG. 6. Diagrammatic representation of the splitting functions in Eqs. (16) and (20).

The first line describes the splitting in flavor space, the distribution of the Z_+ variable and the distribution of the modulus of the transverse momentum \mathbf{k}_{2T} of q_2 , while the second line gives the distribution of the azimuthal angle $\phi_{\mathbf{k}_2}^{q_1}$ of \mathbf{k}_{2T} . The azimuthal angle $\phi_{\mathbf{k}_2}^{q_1}$ is measured in the QHF. The azimuthal distribution of \mathbf{k}_2 has a modulation whose amplitude depends on the correlation coefficients of the string end points times the analyzing power \hat{a} [see Eq. (17)]. The latter is given by

$$\hat{a}(\mathbf{k}_{2T}) = \frac{2\text{Im}(\mu) \mathbf{k}_{2T}}{|\mu|^2 + \mathbf{k}_{2T}^2}. \quad (18)$$

To recall the meaning of \hat{a} , we consider the fragmentation of a quark with polarization vector $\mathbf{S}_{q_1} = (\mathbf{S}_{q_1T}, \mathbf{S}_{q_1L})$, where \mathbf{S}_{q_1T} and \mathbf{S}_{q_1L} are the transverse and longitudinal polarizations with respect to the string axis. As shown in Ref. [27], the splitting function for the emission of a PS meson has a similar expression as Eq. (17) but the third line is substituted with $1 - \hat{a} \mathbf{S}_{q_1T} \cdot \hat{\mathbf{k}}_{2T}$. The distribution of the azimuthal angle of \mathbf{k}_{2T} is characterized by the modulation $\sin(\phi_{\mathbf{k}_2}^{q_1} - \phi_{\mathbf{S}_{q_1T}})$, which is transferred to the hadron and is responsible for the Collins effect. Comparing with Eq. (17), one can see that the coefficients $\mathcal{C}_{x0}^{q_1 \bar{q}_1}$ and $\mathcal{C}_{y0}^{q_1 \bar{q}_1}$ play the role of the x and y components of the transverse polarization vector \mathbf{S}_{q_1T} . Note however that due to Eq. (11) these coefficients are zero for the primary quark-antiquark pair $q_1 \bar{q}_1$, so the last line of Eq. (17) is just equal to unity. This will be no more the case in the iterations, i.e. after the first quark or antiquark splitting.

Vector meson emission. If the quark end of the string emits a VM instead of a PS meson, the acceptance matrix $\eta(q_1)$ is more explicitly represented by the diagram of Fig. 3 than by the rectangle B in Fig. 1. This diagram represents the probability of the process $q_1 \rightarrow h = \text{VM} + q_2$. The splitting matrix in Eq. (12) can be decomposed as $T_{q_2, h = \text{VM}, q_1}^a \mathbf{V}_a$ and the VM coupling in Eq. (13) as $\Gamma^a \mathbf{V}_a$, where the label $a = x, y, z$ indicates the components of the polarization vector \mathbf{V} of the VM in the QHF.

Following Fig. 3, the acceptance matrix $\eta(q_1)$ after the emission of a VM can be written as

$$\eta(q_1) = T_{q_2, h=VM, q_1}^{\dagger a'} \eta(q_2) T_{q_2, h=VM, q_1}^a D_{a', a}, \quad (19)$$

where the matrix D with elements $D_{a'a} = \langle a' | D | a \rangle$ is the decay matrix that implements the information about the decay products of the VM (see Sec. III A 2). The decay matrix is an acceptance matrix that replaces the trivial one $\eta(h) = 1$ of the PS case. If the decay of the meson is not analyzed or the angular distribution of the decay products is integrated over, the decay matrix is the identity matrix $D_{a'a} = \delta_{a'a}$.

Inserting Eq. (19) in Eq. (2), the probability distribution for the emission of a VM from the quark end of the string is obtained by taking $\eta(\bar{q}_1) = 1^{\bar{q}_1}$ and $\eta(q_2) = 1^{q_2}$. This leads to the probability distribution for a nonanalyzed VM:

$$\begin{aligned} & \frac{dP(q_1 \rightarrow h = VM + q_2; q_1 \bar{q}_1)}{dM^2 dZ_+ Z_+^{-1} d^2 \mathbf{p}_T} \\ & \equiv F_{q_2, h, q_1}(M^2, Z_+, \mathbf{p}_T; \mathbf{k}_{1T}, \mathcal{C}^{q_1 \bar{q}_1}) \\ & = \text{Tr}_{q_2 \bar{q}_1} [\mathbf{T}_{q_2, h=VM, q_1}^a \rho(q_1, \bar{q}_1) \mathbf{T}_{q_2, h=VM, q_1}^{\dagger a'}], \quad (20) \end{aligned}$$

where we have defined $\mathbf{T}_{q_2, h=VM, q_1}^a = T_{q_2, h=VM, q_1}^a \otimes 1^{\bar{q}_1}$. Equation (20) is represented by the diagram in Fig. 6. Compared to the PS case in Eq. (17), the splitting function for VM emission depends additionally on the invariant mass squared M^2 of the meson, which is not fixed. The invariant mass is included also in the phase space factor to account for the mass distribution of the resonance. As indicated in the third line in Eq. (20) a summation over the polarization states of the VM is understood.

Inserting in Eq. (20) the splitting matrix (12) with the VM coupling (13) and \hat{u}_{q_1} from (14), we obtain the following expression for the splitting function for VM emission:

$$\begin{aligned} & F_{q_2, h=VM, q_1}(M^2, Z_+, \mathbf{p}_T; \mathbf{k}_{1T}, \mathcal{C}^{q_1 \bar{q}_1}) \\ & = \frac{\hat{u}_{q_1, h}}{\hat{u}_{q_1}} |D_h(M^2)|^2 \left(\frac{1 - Z_+}{\varepsilon_h^2} \right)^a e^{-b_L \varepsilon_h^2 / Z_+} N_a^{-1}(\varepsilon_h^2) \\ & \times f_T^2(\mathbf{k}_{2T}) \frac{|\mu|^2 + \mathbf{k}_{2T}^2}{|\mu|^2 + \langle \mathbf{k}_T^2 \rangle_{f_T}} (1 - \hat{a}(\mathbf{k}_{1T}) f_L \mathcal{C}_{x0}^{q_1 \bar{q}_1} \sin \phi_{\mathbf{k}_2}^{q_1} \\ & + \hat{a}(\mathbf{k}_{1T}) f_L \mathcal{C}_{y0}^{q_1 \bar{q}_1} \cos \phi_{\mathbf{k}_2}^{q_1}). \quad (21) \end{aligned}$$

The structure of the splitting function and the meaning of the different pieces is the same as in the PS meson case in Eq. (17). The differences are the introduction of the invariant mass distribution $|D_h(M^2)|^2$ and the amplitudes of the modulations in the azimuthal angle $\phi_{\mathbf{k}_2}^{q_1}$ in the third and last lines. As shown in Ref. [27], for VM production the amplitudes of the modulations in the distribution of $\phi_{\mathbf{k}_2}^{q_1}$

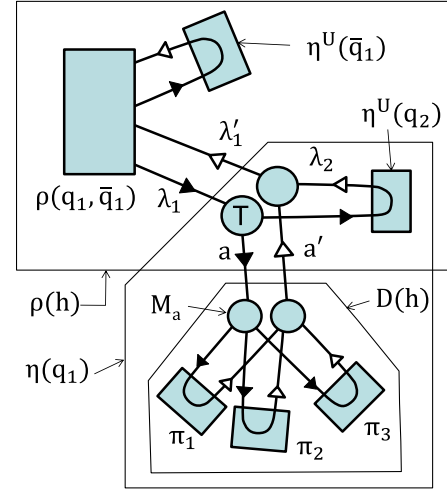


FIG. 7. Unitarity diagram for $q_1 \bar{q}_1 \rightarrow hX$, where h is a VM emitted from q_1 and decays in three pions. Particularly is shown the decay matrix of the VM.

are the opposite to those of the PS case, and they are reduced by the factor f_L [cf. with the last line in Eq. (17)].

2. The polarized decay of the vector meson

The VM has been emitted. Now we consider its decay. The spin-density matrix of h can be calculated by inserting Eq. (19) in Eq. (2), imposing $\eta(\bar{q}_1) = 1^{\bar{q}_1}$ and $\eta(q_2) = 1^{q_2}$, and freeing the polarization indices of the meson. The result is

$$\begin{aligned} \rho_{aa'}(h) & = \frac{\text{Tr}_{q_2 \bar{q}_1} [\mathbf{T}_{q_2, h=VM, q_1}^a \rho(q_1, \bar{q}_1) \mathbf{T}_{q_2, h=VM, q_1}^{\dagger a'}]}{\text{Tr}[\dots]} \\ & = \frac{\mathcal{C}_{a0}^{q_1 \bar{q}_1} \text{Tr}_q [\Delta(\mathbf{k}_{2T}) \Gamma^a(h) \sigma_a^{q_1} \Gamma^{a' \dagger}(h) \Delta^\dagger(\mathbf{k}_{2T})]}{\text{Tr}[\dots]} \quad (22) \end{aligned}$$

and is represented by the upper rectangular domain in Fig. 7. In the denominator [...] indicates the same expression as in the numerator but the trace is taken also on the polarization index a of the VM. a and a' can take the values x, y, z and span the polarization states of the meson measured in the meson rest frame.⁵ We have also used the vector of couplings matrices $\Gamma^a(h) = (G_T \sigma_x^{q_1} \sigma_z^{q_1}, G_T \sigma_y^{q_1} \sigma_z^{q_1}, G_L 1^{q_1})$ [see Eq. (13)].

The spin-density matrix of the VM is used for the generation of the anisotropic angular distribution of the hadrons produced in the decay of the meson. Indicating with $\mathcal{M}_a(p_1, p_2, \dots)$ the matrix element that describes the decay process $VM \rightarrow p_1, p_2, \dots$, the angular distribution of the decay products in the rest frame of the VM can be obtained by

⁵This rest frame is obtained from the c.m.s. by the boost composition of Ref. [27].

$$\frac{d\mathcal{N}}{d\Phi(p_1, p_2, \dots)} = \frac{\mathcal{M}_a(p_1, p_2, \dots)\rho_{aa'}(h)\mathcal{M}_{a'}^\dagger(p_1, p_2, \dots)}{\int d\Phi(p_1, p_2, \dots)[\dots]}. \quad (23)$$

The quantity $d\Phi(p_1, p_2, \dots)$ indicates the differential phase space element involved in the decay. The detailed description of the decay processes included in the string + 3P_0 model is given in Ref. [27]. The quantities in the numerator on the rhs of Eq. (23) are represented in Fig. 7 for the example $h = \omega \rightarrow 3\pi$.

Following the CK recipe, the decay process of the VM fixes the decay matrix $D(\hat{p}_1, \hat{p}_2, \dots)$, where $\hat{p}_1, \hat{p}_2, \dots$ are the generated four-momenta of the decay hadrons. The decay matrix is necessary to account for the quantum mechanical correlations between the orientation of the decay hadrons and the spin state of the leftover quark q_2 or the antiquark \bar{q}_1 . It is given by

$$D_{a'a}(\hat{p}_1, \hat{p}_2, \dots) = \mathcal{M}_{a'}^\dagger(\hat{p}_1, \hat{p}_2, \dots)\mathcal{M}_a(\hat{p}_1, \hat{p}_2, \dots), \quad (24)$$

and hence it is evaluated at the generated momenta of the decay hadrons and depends on the matrix element that describes the decay process. The formation of the decay matrix is represented in Fig. 7 by the hexagonal domain.

3. Propagation of the spin correlations

After the emission of the hadron h from the quark end of the string by the splitting $q_1 \rightarrow h + q_2$ the string piece stretched between q_2 and \bar{q}_1 remains to be fragmented. The $q_2\bar{q}_1$ string is characterized by a new joint spin-density matrix $\rho(q_2, \bar{q}_1)$ and associated new correlation coefficients $C^{q_2\bar{q}_1}$. If $h = \text{PS}$, the joint spin-density matrix can be calculated by inserting in Eq. (2) the acceptance matrix $\eta(q_1)$ in Eq. (4b) and identifying the resulting expression with $d\sigma \propto \text{Tr}_{q_2\bar{q}_1}[\rho(q_2, \bar{q}_1)\eta(q_2) \otimes \eta(\bar{q}_1)]$. If $h = \text{VM}$, the acceptance matrix to be used is that in Eq. (19) with the decay matrix in Eq. (24). We obtain (given the emission of the hadron h from the quark end of the string) for the joint spin-density matrix of the system $q_2\bar{q}_1$

$$\rho(q_2, \bar{q}_1) = \begin{cases} \mathbf{T}_{q_2, h, q_1}\rho(q_1, \bar{q}_1)\mathbf{T}_{q_2, h, q_1}^\dagger / \text{Tr}[\dots] & h = \text{PS}, \\ \mathbf{T}_{q_2, h, q_1}^a\rho(q_1, \bar{q}_1)\mathbf{T}_{q_2, h, q_1}^{\dagger a'} D_{aa'} / \text{Tr}[\dots] & h = \text{VM}. \end{cases} \quad (25)$$

It is represented by the domain C in Fig. 1. The associated correlation coefficients are

$$\begin{aligned} C_{\alpha\beta}^{q_2\bar{q}_1} &= \text{Tr}_{q_2\bar{q}_1}(\rho(q_2, \bar{q}_1)\sigma_{\alpha'}(q) \otimes \sigma_{\beta}(\bar{q}_1)) \\ &= C_{\alpha\beta}^{q_1\bar{q}_1} M_{\alpha\alpha'}^{q_1} / C_{\alpha\beta}^{q_1\bar{q}_1} M_{\alpha\alpha'}^{q_1}. \end{aligned} \quad (26)$$

Thus the correlation coefficients $C^{q_2\bar{q}_1}$ can be obtained by matrix operations on the correlation coefficients $C^{q_1\bar{q}_1}$ by

introducing the matrix $M_{\alpha\alpha'}^{q_1}$. Such matrix for PS and VM emissions is given by

$$\begin{aligned} M_{\alpha\alpha'}^{q_1}|_{\text{PS}} &= \frac{1}{2} \text{Tr}[\sigma_{\alpha'}^{q_1} \Delta(\mathbf{k}_{2T}) \Gamma_h \sigma_{\alpha}^{q_1} \Gamma_h^\dagger \Delta^\dagger(\mathbf{k}_{2T})], \\ M_{\alpha\alpha'}^{q_1}|_{\text{VM}} &= \frac{1}{2} \text{Tr}[\sigma_{\alpha'}^{q_1} \Delta(\mathbf{k}_{2T}) \Gamma^a(h) \sigma_{\alpha}^{q_1} \Gamma^{\dagger a'}(h) \Delta^\dagger(\mathbf{k}_{2T})] D_{a'a}. \end{aligned} \quad (27)$$

4. Hadron emission from the antiquark end

Pseudoscalar meson emission. The emission of a hadron H from the antiquark end of the string by the splitting $\bar{q}_1 \rightarrow H + \bar{q}_2$, after the hadron h was emitted from the quark end proceeds in a way symmetrical to that of the emission of h . The emission of h , which has already occurred, has changed the $q_1 - \bar{q}_1$ string in the $q_2 - \bar{q}_1$ one and we must take into account the spin information coming from the splitting $q_1 \rightarrow h + q_2$. This information is contained in the spin-density matrix $\rho(q_2, \bar{q}_1)$ of Eq. (25). Therefore, to get the momentum spectrum of H in the PS case it suffices to make in Eq. (16) the replacement $q_1 \rightarrow \bar{q}_1$, $\bar{q}_1 \rightarrow q_2$ and $q_2 \rightarrow \bar{q}_2$, $h \rightarrow H$, $Z_+ \rightarrow Z_-$ and $\mathbf{p}_T \rightarrow \mathbf{P}_T$. We obtain

$$\begin{aligned} &\frac{dP(\bar{q}_1 \rightarrow H = \text{PS} + \bar{q}_2; q_2\bar{q}_1)}{dZ_- Z_-^{-1} d^2\mathbf{P}_T} \\ &\equiv F_{\bar{q}_2, H, \bar{q}_1}(Z_-, \mathbf{P}_T; \bar{\mathbf{k}}_{1T}, C^{q_2\bar{q}_1}) \\ &= \text{Tr}_{q_2\bar{q}_2}[\mathbf{T}_{\bar{q}_2, H, \bar{q}_1}\rho(q_2, \bar{q}_1)\mathbf{T}_{\bar{q}_2, H, \bar{q}_1}^\dagger], \end{aligned} \quad (28)$$

where we have defined $\mathbf{T}_{\bar{q}_2, H, \bar{q}_1} = 1^{q_2} \otimes T_{\bar{q}_2, H, \bar{q}_1}$, and the joint spin-density matrix $\rho(q_2, \bar{q}_1)$ is given in Eq. (25). The splitting function $F_{\bar{q}_2, H = \text{PS}, \bar{q}_1}$ depends on Z_- , \mathbf{P}_T , $\bar{\mathbf{k}}_{1T}$ and on the correlation coefficients $C^{q_2\bar{q}_1}$, calculated in Eq. (26). It gives the conditional probability of emitting the hadron H , given that the hadron h was emitted from the quark end.

Inserting in Eq. (28) the splitting matrix in Eq. (15), the explicit expression for $F_{\bar{q}_2, H = \text{PS}, \bar{q}_1}$ is

$$\begin{aligned} &F_{\bar{q}_2, H = \text{PS}, \bar{q}_1}(Z_-, \mathbf{P}_T; \bar{\mathbf{k}}_{1T}, C^{q_2\bar{q}_1}) \\ &= \frac{\hat{u}_{\bar{q}_1, H}}{\hat{u}_{\bar{q}_1}} \left(\frac{1 - Z_-}{\varepsilon_H^2} \right)^a e^{-b_L \varepsilon_H^2 / Z_-} N_a^{-1} (\varepsilon_H^2) f_T^2(\bar{\mathbf{k}}_{2T}^2) \frac{|\mu|^2 + \bar{\mathbf{k}}_{2T}^2}{|\mu|^2 + \langle \mathbf{k}_T^2 \rangle_{f_T}} \\ &\quad \times (1 + \hat{a}(\bar{\mathbf{k}}_{2T}) C_{0x}^{q_2\bar{q}_1} \sin\phi_{\bar{\mathbf{k}}_2}^{\bar{q}_1} - \hat{a}(\bar{\mathbf{k}}_{2T}) C_{0y}^{q_2\bar{q}_1} \cos\phi_{\bar{\mathbf{k}}_2}^{\bar{q}_1}). \end{aligned} \quad (29)$$

This expression is similar to Eq. (17), with the substitutions $Z_+ \rightarrow Z_-$, $\{\mathbf{k}_{1T}, \mathbf{p}_T, \mathbf{k}_{2T}\} \rightarrow \{\bar{\mathbf{k}}_{1T}, \mathbf{P}_T, \bar{\mathbf{k}}_{2T}\}$, $\phi_{\bar{\mathbf{k}}_2}^{q_1} \rightarrow \phi_{\bar{\mathbf{k}}_2}^{\bar{q}_1}$ and $C^{q_1\bar{q}_1} \rightarrow C^{q_2\bar{q}_1}$. The azimuthal angle $\phi_{\bar{\mathbf{k}}_2}^{\bar{q}_1}$ of the transverse momentum $\bar{\mathbf{k}}_{2T}$ of \bar{q}_2 is measured in the AHF. The azimuthal angle in the QHF can be obtained using Eq. (9). Equation (29) is responsible for a Collins effect for the production of H in the AHF. The strength of the effect depends on the emission of h from the quark side

through the correlation coefficients $C^{q_2\bar{q}_1}$. A similar Collins effect would have been found if we had treated the emission of h after that of H . In fact, these effects are related and they sum up to an azimuthal correlation between \mathbf{p}_T and \mathbf{P}_T given by Eq. (38).

Vector meson emission. The splitting function for the emission of a VM in the antiquark splitting $\bar{q}_1 \rightarrow H = \text{VM} + \bar{q}_2$ can be obtained from Eq. (28) by the substitution $1^{q_1} \otimes T_{\bar{q}_2, h=PS, \bar{q}_1} \otimes 1^{q_1} \otimes T_{\bar{q}_2, h=VM, \bar{q}_1}^a \mathbf{V}_a$ and by summing over the polarization states of the meson. The corresponding splitting function takes the explicit form

$$\begin{aligned} F_{\bar{q}_2, H=VM, \bar{q}_1}(M^2, Z_-, \mathbf{P}_T; \bar{\mathbf{k}}_{1T}, C^{q_2\bar{q}_1}) \\ = \frac{\hat{u}_{\bar{q}_1, H}}{\hat{u}_{\bar{q}_1}} |D_H(M^2)|^2 \left(\frac{1-Z_-}{\varepsilon_H^2} \right)^a e^{-b_L \varepsilon_H^2 / Z_-} N_a^{-1} (\varepsilon_H^2) \\ \times f_T^2(\bar{\mathbf{k}}_{2T}^2) \frac{|\mu|^2 + \bar{\mathbf{k}}_{2T}^2}{|\mu|^2 + \langle \mathbf{k}_T^2 \rangle_{f_T}} (1 - \hat{a}(\bar{\mathbf{k}}_{2T}) f_L C_{0x}^{q_2\bar{q}_1} \sin \phi_{\bar{\mathbf{k}}_2}^{\bar{q}_1} \\ + \hat{a}(\bar{\mathbf{k}}_{2T}) f_L C_{0y}^{q_2\bar{q}_1} \cos \phi_{\bar{\mathbf{k}}_2}^{\bar{q}_1}). \end{aligned} \quad (30)$$

We note again that the azimuthal angle $\phi_{\bar{\mathbf{k}}_2}^{\bar{q}_1}$ of the transverse momentum of \bar{q}_2 is measured in the AHF.

The density matrix of H as well as the correlation coefficients of the new string piece after the antiquark splitting $\bar{q}_1 \rightarrow H + \bar{q}_2$ have similar expressions to those that are obtained when the hadron is emitted from the quark side (see Secs. III A 2 and III A 3). The calculation is not repeated here and the explicit expressions can be found in Appendix B.

5. End of the fragmentation chain

We assume that several hadrons have been emitted from both string ends and that a string piece stretched between a quark q_l and an antiquark \bar{q}_n remains to be fragmented by the process $q_l \bar{q}_n \rightarrow h + H$. Following the recipe adopted in the MC implementation of the Lund model of string fragmentation [28], the condition for the termination of the fragmentation chain is called if the squared mass of the $q_l \bar{q}_n$ string falls below some minimum value M_{\min}^2 of the order of a GeV (for the precise definition of M_{\min}^2 see Ref. [28]). The fragmentation chain is thus ended by the creation of a last quark pair and the formation of the hadrons h and H . The corresponding spacetime picture is shown in Fig. 8(a).

To construct these two hadrons we use the following recipe. We consider the reaction $q_l + \bar{q}_n \rightarrow h + H$ equally as $q_l \rightarrow h + q_{l+1}$ followed by $q_{l+1} \rightarrow H + q_{l+2}$, as shown in Fig. 8(b), or as $\bar{q}_n \rightarrow \bar{H} + q_{n+1}$ followed by $\bar{q}_{n+1} \rightarrow h + q_{n+2}$, where \bar{q}_n , \bar{q}_{n+1} and \bar{q}_{n+2} are, respectively, the antiparticles of q_{l+2} , q_{l+1} and q_l . The $q_l \bar{q}_n$ pair is characterized by the joint spin-density matrix $\rho(q_l, \bar{q}_n) = 4^{-1} C_{\mu\nu}^{q_l \bar{q}_n} \sigma_\mu^{q_l} \otimes \sigma_\nu^{\bar{q}_n}$. If q_l was generated after \bar{q}_n , Eqs. (25)

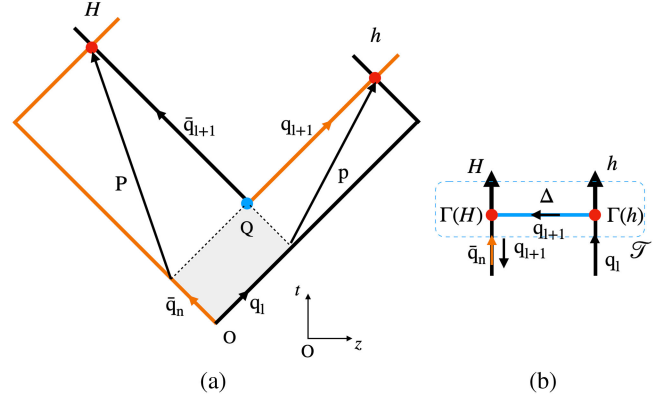


FIG. 8. (a) Spacetime picture of the string fragmentation of the $q_l \bar{q}_n$ pair and the production of the last two hadrons h and H . (b) Associated amplitude for the two-step process $q_l \rightarrow h + q_{l+1}$ and $q_{l+1} \rightarrow H + q_{l+2}$.

and (26) are used to calculate such matrix; otherwise, Eqs. (B2) and (B3) are used. q_l , μ , \bar{q}_n , and ν take the place of q_2 , α' , \bar{q}_1 , and β in the first case, respectively, and of q_2 , α , \bar{q}_2 and β' in the second case.

Starting with $\rho(q_l, \bar{q}_n)$, we build the matrix $R(q_l, q_{l+2})$ obtained by the successive transformations:

- change the signs of $C_{\mu y}^{q_l \bar{q}_n}$ and $C_{\mu z}^{q_l \bar{q}_n}$ (to put everything in the QHF frame),
- reverse the signs of $C_{\mu i}^{q_l \bar{q}_n}$ for $i = x, y$ or z ,
- multiply the resulting matrix on the left and on the right by $1 \otimes \sigma_z$.⁶

To fix the hadron h and H , we draw the flavor u , d or s of q_{l+1} with respective probabilities proportional to \hat{u}_u , \hat{u}_d or \hat{u}_s [see Eq. (14)]. Then the hadron species are drawn with probabilities proportional to $|C_{q_{l+1}, h, q_l}|^2$ and $|C_{q_{l+2}, H, q_{l+1}}|^2$. The mass of VMs is generated according to the corresponding distribution $|D(M^2)|^2$.

To build the four-momenta of p of h and P of H , it is necessary to know the transverse momentum $\mathbf{k}_T(q_{l+1})$ of q_{l+1} . The latter is generated with the probability proportional to

$$\langle j | \mathcal{T}^{a,b} | i \rangle \langle i \otimes j' | R | i' \otimes j \rangle \langle j' | \mathcal{T}^{\dagger a,b} | i' \rangle \quad (31)$$

(summed over repeated indices), where i, j, a and b are spin states of q_l, q_{l+2}, h and H , and

$$\mathcal{T}^{a,b} = \Gamma^b(H) \Delta(\mathbf{k}_T(q_{l+1})) \Gamma^a(h). \quad (32)$$

⁶Steps (b) and (c) come from the expression $\xi(\mathbf{S}) = \sigma_z \chi(-\mathbf{S})$ of an antiquark spinor in the string $+^3P_0$ model [25], where $\chi(\mathbf{S})$ and $\xi(\mathbf{S})$ are the 2D reductions of the Dirac spinors $u(\mathbf{p}, \mathbf{S})$ and $v(\mathbf{p}, \mathbf{S}) = \gamma_5 u(\mathbf{p}, -\mathbf{S})$ in the $\langle \alpha_z \rangle = +1$ subspace. The choice of this subspace is motivated by the relation $\langle \alpha_z \rangle = v_z$ and the fact that in Fig. 8 a longitudinal velocity $v_z = +1$ is attributed to the antiquark just before it reaches the emission vertex of H .

The latter amplitude is also shown in Fig. 8(b). The transverse momenta of the emitted hadrons then calculated as $\mathbf{p}_T = \mathbf{k}_T(q_l) - \mathbf{k}_T(q_{l+1})$ and $\mathbf{P}_T = \mathbf{k}_T(q_{l+1}) - \mathbf{k}_T(q_{l+2})$.

Finally, the longitudinal momenta (and the energies) of the final two hadrons are obtained by calculating the two possible solutions of the system:

$$\begin{aligned} p^+ p^- &= m_h^2 + \mathbf{P}_T^2, \\ (P_{\text{rem}}^+ - p^+)(P_{\text{rem}}^- - p^-) &= m_H^2 + \mathbf{P}_T^2, \end{aligned} \quad (33)$$

with $P_{\text{rem}} = k(q_l) + k(\bar{q}_n) = k(q_l) - k(q_{l+2})$, and choosing one of them, each having a relative weight proportional to $\exp\{-b_L P^+ p^-\}$. The factor $P^+ p^-$ is the area in the past light cone of the spacetime point Q in Fig. 8(a). The exponential gives the probability that no string breaking occurred in the past light cone of Q .

If h and H are VMs, their spin states are described by the joint density matrix of h and H :

$$\begin{aligned} \langle a, b | \rho(h, H) | a', b' \rangle \\ \propto \langle j | T^{a,b} | i \rangle \langle i \otimes j' | R | i' \otimes j \rangle \langle j' | T^{\dagger a', b'} | i' \rangle. \end{aligned} \quad (34)$$

If only h is a VM, one gets the single density matrix $\langle a | \rho(h) | a' \rangle$ by omitting the indices b and b' . The case where only H is a VM is analogous. If h is a VM, its decay is treated like in Sec. III A 2 with $\rho(h) = \text{Tr}_H \rho(h, H)$. If H is also a VM, to generate its decay one must first calculate the decay matrix $D(h)$ as in Sec. III A 2 according to the CK recipe and then decay H according to the density matrix

$$\langle b | \rho(H) | b' \rangle \propto \langle a, b | \rho(h, H) | a', b' \rangle \langle a' | D(h) | a \rangle. \quad (35)$$

The proposed recipe is formulated at the amplitude level, and it can be regarded as the generalization of the recipe of the Lund model [28] employed for the joining of the quark and antiquark jets in Monte Carlo simulations.

B. The recursive recipe for the string fragmentation

By gathering the ingredients presented in Sec. III A, we can now formulate the following recipe for the fragmentation of a string stretched between a quark q_1 and an antiquark \bar{q}_1 with entangled spin states. As already mentioned, we assume the $q_1 \bar{q}_1$ pair to be produced in the hard process $e^+ e^- \rightarrow \gamma^* \rightarrow q_1 \bar{q}_1$. The recipe is however general and can be applied to other processes as well. In fact, the information on the hard process that produces the pair is included only in the joint spin-density matrix $\rho(q_1, \bar{q}_1)$, which is required as an initial condition for the simulation of the hadronization process $q_1 \bar{q}_1 \rightarrow h_1, h_2, \dots, h_N$.

We divide the simulation of the $e^+ e^-$ annihilation in the generation of the primary quark pair and in the string fragmentation of the pair.

1. Generation of the primary quark pair

Generate the flavor of q_1 using the relative probabilities $\hat{P}(u\bar{u}) : \hat{P}(d\bar{d}) : \hat{P}(s\bar{s}) : \hat{P}(c\bar{c}) : \dots$, where $\hat{P}(q_1 \bar{q}_1) = \hat{\sigma}(q_1 \bar{q}_1) / \sum_q \hat{\sigma}(q\bar{q})$ and $\hat{\sigma} = \int d\cos\theta d\hat{\sigma} / d\cos\theta$ is the integrated hard cross section obtained using Eq. (7). Then generate the polar angle θ using the probability distribution obtained by the cross section ratio $\hat{\sigma}^{-1} d\hat{\sigma} / d\hat{\Omega}$. Set up the four-momenta of e^+ , e^- , q_1 and \bar{q}_1 using Eq. (6) and use the generated value of θ to calculate the correlation coefficients $\mathcal{C}^{q_1 \bar{q}_1}$. The latter can be read from the expression of the joint spin-density matrix of the $q_1 \bar{q}_1$ pair in Eq. (10).

2. String fragmentation of the quark pair

The initial conditions for the string fragmentation process are the momenta k_1 of q_1 and \bar{k}_1 of \bar{q}_1 and the joint density matrix $\rho(q_1, \bar{q}_1)$. From the quark momenta we define the available light-cone momenta $P_{\text{tot}}^+ = \sqrt{s} = P_{\text{tot}}^-$, where $P_{\text{tot}} = k_1 + \bar{k}_1$. It is $\mathbf{k}_{1T} = \bar{\mathbf{k}}_{1T} = \mathbf{0}$, and thus $\mathbf{P}_{\text{tot},T} = \mathbf{0}$. To generate recursively the string fragmentation process of the $q_1 \bar{q}_1$ pair, repeat the following steps:

- (1) Select with equal probability whether to emit the first hadron h from the quark side or the anti-quark side.⁷
- (2) If the splitting is performed from the quark side: select a new quark pair $q_2 \bar{q}_2$ with probability $\hat{u}_{q_1, h} / \hat{u}_{q_1}$ using Eq. (14), form the hadron $h = (q_1 \bar{q}_2)$ and decide whether it is a VM with probability f_{VM} , or a PS meson. If h is a PS meson, generate \mathbf{k}_{2T}^+ , $\phi_{\mathbf{k}_2}^{q_1}$ and Z_+ using the splitting function $F_{q_2, h=\text{PS}, q_1}(Z_+, \mathbf{p}_T; \mathbf{k}_{1T}, \mathcal{C}^{q_1 \bar{q}_1})$ in Eq. (17). If h is a VM, use instead the splitting function $F_{q_2, h=\text{VM}, q_1}(M^2, Z_+, \mathbf{p}_T; \mathbf{k}_{1T}, \mathcal{C}^{q_1 \bar{q}_1})$ in Eq. (21) to generate first the invariant mass squared M^2 and then \mathbf{k}_{2T}^+ , $\phi_{\mathbf{k}_2}^{q_1}$ and Z_+ . Calculate the light-cone momenta $p^+ = Z_+ k_1^+$ and $p^- = \varepsilon_h^2 / p^+$, the new available light-cone momenta $(P_{\text{tot}}^+)^{\text{new}} = P_{\text{tot}}^+ - p^+$ and $(P_{\text{tot}}^-)^{\text{new}} = P_{\text{tot}}^- - \varepsilon_h^2 / p^+$, and the transverse momentum $\mathbf{P}_{\text{tot},T}^{\text{new}} = \mathbf{P}_{\text{tot},T} - \mathbf{p}_T$. If $(P_{\text{tot}}^+)^{\text{new}} < M_{\text{min}}^2$, go to step 4. Otherwise set $P_{\text{tot}} = (P_{\text{tot}}^+)^{\text{new}}$ and continue by constructing the four-momentum of h using $p = (E_h, \mathbf{p}_T, p_L)$, where $E_h = (p^+ + p^-) / 2$ and $p_L = (p^+ - p^-) / 2$.

If h is a VM, apply the following further steps to decay the meson:

- (2.1) Calculate the spin-density matrix of h using Eq. (22) and generate the momenta of the decay hadrons in the rest frame of h using Eq. (23). The expressions for the decay amplitude \mathcal{M}_a can be found in Ref. [27].
- (2.2) Calculate the decay matrix D using Eq. (24).

⁷As done in the Lund string model [28].

(2.3) To come back to the center of mass frame, apply the composition of longitudinal and transverse boosts in Ref. [27] to the decay hadrons.

- (3) Calculate the correlation coefficients $\mathcal{C}^{q_2\bar{q}_1}$ of the new string piece with end points q_2 and \bar{q}_1 using Eqs. (26) and (27). Let q_2, k_2 and $\mathcal{C}^{q_2\bar{q}_1}$ take the place of q_1, k_1 and $\mathcal{C}^{q_1\bar{q}_1}$, respectively, and go to step 1.

If the splitting is performed from the antiquark side: the steps are similar to the splitting from the quark side and can be found in Appendix C.

- (4) The mass of the remaining string piece $q_l - \bar{q}_n$ has become less than M_{\min} . To terminate the fragmentation chain hadronize the remaining $q_l\bar{q}_n$ pair by generating the last quark pair $q_{l+1}\bar{q}_{l+1}$ and forming the hadrons $h = (q_l\bar{q}_{l+1})$ and $H = (\bar{q}_n q_{l+1})$. For each hadron, decide whether it is a VM with probability f_{VM} or a PS meson. Generate the longitudinal splitting variable and transverse momentum of q by the recipe in Sec. III A 5. Calculate the transverse momenta $\mathbf{p}_T = \mathbf{k}_{lT} - \mathbf{k}_T(q_{l+1})$ and $\mathbf{P}_T = \bar{\mathbf{k}}_{nT} + \mathbf{k}_T(q_{l+1})$. Finally build the four-momentum p of h and P of H .

Steps 1–4 are similar to those applied for the implementation of the Lund string model in the PYTHIA event generator [21,22]. In addition the CK recipe and the rules of the string $+^3P_0$ model are used to account for the spin correlations at each hadron emission and to propagate these correlations after each emission as required by quantum mechanics. This recursive recipe is therefore suitable for the implementation of the e^+e^- annihilation with spin effects in MCEGs. The natural choice would be the implementation in PYTHIA 8 [22] by extending the StringSpinner package [24], which currently is applied only to the polarized SIDIS process.

IV. APPLICATION TO BACK-TO-BACK HADRON PRODUCTION IN e^+e^-

The recipe for the fragmentation of a string stretched between a quark pair with correlated spin states described in Sec. III A can be checked to reproduce the expected azimuthal distribution by applying it to the process $e^+e^- \rightarrow hHX$. As in Sec. III A, we assume h to be emitted in the splitting $q_1 \rightarrow h + q_2$ and H to be emitted in the splitting $\bar{q}_1 \rightarrow H + \bar{q}_2$. The two hadrons are associated to different quark jets and are thus expected to be produced nearly back to back in the c.m.s. The calculations are shown in Sec. IV A for the case $h = \text{PS}$ and $H = \text{PS}$ and in Sec. IV B for the case $h = \text{VM}$ and $H = \text{PS}$. For these calculations we neglect the quark mass m_q .

A. Production of back-to-back PS mesons

According to the recipe described in Sec. III A, the probability of producing the two hadrons h and H is

obtained as a three-step process (e.g., starting the string fragmentation from the q_1 side): (i) the production of the $q_1\bar{q}_1$ pair in the hard process $e^+e^- \rightarrow q_1\bar{q}_1$, (ii) the splitting $q_1 \rightarrow h + q_2$ given the $\mathcal{C}^{q_1\bar{q}_1}$ correlation coefficients, and (iii) the splitting $\bar{q}_1 \rightarrow H + \bar{q}_2$ given the correlation coefficients $\mathcal{C}^{q_2\bar{q}_1}$. The probability for step (i) to occur is given by the cross section for the hard scattering. The probabilities for steps (ii) and (iii) to occur are given by the splitting functions of Eqs. (17) and (29), respectively. The total probability is the product of the three probabilities, and it can be written as [cf. Eq. (1) with $\eta(q_2) = 1^{q_2}$ and $\eta(\bar{q}_2) = 1^{\bar{q}_2}$]

$$\begin{aligned} dP(e^+e^- \rightarrow hHX) &= \hat{\sigma}^{-1} \frac{d\hat{\sigma}}{d\cos\theta} d\cos\theta \\ &\times F_{q_2,h,q_1}(Z_+, \mathbf{p}_T; \mathbf{k}_{lT}, \mathcal{C}^{q_1\bar{q}_1}) Z_+^{-1} dZ_+ d^2\mathbf{p}_T \\ &\times F_{\bar{q}_2,H,\bar{q}_1}(Z_-, \mathbf{P}_T; \bar{\mathbf{k}}_{lT}, \mathcal{C}^{q_2\bar{q}_1}) Z_-^{-1} dZ_- d^2\mathbf{P}_T, \end{aligned} \quad (36)$$

where $\mathbf{k}_{lT} = 0$ and $\bar{\mathbf{k}}_{lT} = 0$.

To calculate the splitting function $F_{q_2,h,q_1}(Z_+, \mathbf{p}_T; \mathbf{k}_{lT}, \mathcal{C}^{q_1\bar{q}_1})$ of Eq. (17) one takes $\mathcal{C}_{x0}^{q_1\bar{q}_1} = \mathcal{C}_{y0}^{q_1\bar{q}_1} = 0$, according to Eq. (11). Therefore h is emitted with a flat azimuthal distribution. For the splitting function $F_{\bar{q}_2,H,\bar{q}_1}$ of Eq. (29), instead, the coefficients $\mathcal{C}_{0x}^{q_2\bar{q}_1}$ and $\mathcal{C}_{0y}^{q_2\bar{q}_1}$ are needed. They can be calculated by using Eqs. (26) and (27), with the explicit expressions for the splitting amplitude in Eq. (12) and the quark coupling to PS mesons in Eq. (13). We obtain

$$\begin{aligned} \mathcal{C}_{0x}^{q_2\bar{q}_1} &= \mathcal{C}_{xx}^{q_1\bar{q}_1} \frac{M_{x0}^{q_1}}{M_{00}^{q_1}} = -\frac{\sin^2\theta}{1 + \cos^2\theta} \hat{a}(\mathbf{k}_{2T}) (-\sin\phi_{\mathbf{k}_2}^{q_1}), \\ \mathcal{C}_{0y}^{q_2\bar{q}_1} &= \mathcal{C}_{yy}^{q_1\bar{q}_1} \frac{M_{y0}^{q_1}}{M_{00}^{q_1}} = -\frac{\sin^2\theta}{1 + \cos^2\theta} \hat{a}(\mathbf{k}_{2T}) \cos\phi_{\mathbf{k}_2}^{q_1}, \end{aligned} \quad (37)$$

meaning that the quark \bar{q}_1 has a transverse polarization that depends on the transverse momentum of h . According to Eq. (29), this means that H is emitted with a Collins effect in the AHF.

The hadron transverse momenta are given by $\mathbf{p}_T = -\mathbf{k}_{2T}$ and $\mathbf{P}_T = -\bar{\mathbf{k}}_{2T}$. Indicating by ϕ_h^q and ϕ_H^q the azimuthal angles of \mathbf{p}_T and \mathbf{P}_T in the helicity frame of $q = q_1, \bar{q}_1$, respectively, one has $\phi_h^{q_1} = \phi_{\mathbf{k}_2}^{q_1} + \pi$ and $\phi_H^{\bar{q}_1} = \phi_{\bar{\mathbf{k}}_2}^{\bar{q}_1} + \pi$. The azimuthal angle $\phi_H^{\bar{q}_1}$ can be expressed in the QHF using Eq. (9), and it is $\phi_H^{\bar{q}_1} = \pi - \phi_{\bar{\mathbf{k}}_2}^{\bar{q}_1}$.

With these considerations, and inserting in Eq. (36) the Eqs. (17) and (29) with the coefficients in Eq. (37), we obtain the probability for the PS + PS case

$$\begin{aligned}
\frac{dP(e^+e^- \rightarrow hHX)}{d \cos \theta dZ_+ d^2 \mathbf{p}_T dZ_- d^2 \mathbf{P}_T} &= \frac{3}{8} (1 + \cos^2 \theta) \times \frac{\hat{u}_{q_1, h}}{\hat{u}_{\bar{q}_1}} Z_+^{-1} \left(\frac{1 - Z_+}{\varepsilon_h^2} \right)^a e^{-b_L \varepsilon_h^2 / Z_+} N_a^{-1}(\varepsilon_h^2) f_T^2(\mathbf{p}_T^2) \frac{|\mu|^2 + \mathbf{P}_T^2}{|\mu|^2 + \langle \mathbf{P}_T^2 \rangle_{f_T}} \\
&\times \frac{\hat{u}_{\bar{q}_1, H}}{\hat{u}_{\bar{q}_1}} Z_-^{-1} \left(\frac{1 - Z_-}{\varepsilon_H^2} \right)^a e^{-b_L \varepsilon_H^2 / Z_-} N_a^{-1}(\varepsilon_H^2) f_T^2(\mathbf{P}_T^2) \frac{|\mu|^2 + \mathbf{P}_T^2}{|\mu|^2 + \langle \mathbf{P}_T^2 \rangle_{f_T}} \\
&\times \left(1 + \frac{\sin^2 \theta}{1 + \cos^2 \theta} \hat{a}(p_T) \hat{a}(P_T) \cos(\phi_h^{q_1} + \phi_H^{\bar{q}_1}) \right). \tag{38}
\end{aligned}$$

As can be seen from the last factor of the equation, the recipe produces the azimuthal modulation $\cos(\phi_h^{q_1} + \phi_H^{\bar{q}_1})$ associated to the Collins asymmetry for the production of two back-to-back hadrons in e^+e^- , as calculated in Refs. [5,33]. Also, the amplitude of the modulation has a positive sign, as observed by the BELLE [12] and BABAR [9,10] experiments. The azimuthal angles of both hadrons are referred to the same reference system, which in this case is the QHF. The amplitude of the modulation is proportional to the squared imaginary part $(\text{Im}\mu)^2$ of the complex mass μ . If the $\text{Im}\mu$ vanishes, then the asymmetry vanishes, as is the case for the transverse spin effects in the string + 3P_0 model [25,27].

The simple formula (38) holds only for the two leading hadrons produced in each quark jet. In order to obtain the complete results for the Collins asymmetries in e^+e^- annihilation, the present model must be implemented in a Monte Carlo event generator, either standalone as in Ref. [27] or in the PYTHIA MCEG by extending the StringSpinner package in Ref. [24]. Still, this calculation is important as it demonstrates that the recipe presented in this work reproduces the azimuthal correlation of the hadrons produced in e^+e^- annihilation.

B. Production of back-to-back VM and PS mesons

It is also interesting to study the qualitative prediction of the string + 3P_0 model for the process $e^+e^- \rightarrow hHX$, with $h = \text{VM}$ and $H = \text{PS}$ being produced back to back in the quark and antiquark jets, respectively. This asymmetry has never been measured.

The probability $dP(e^+e^- \rightarrow hHX)$, with $h = \text{VM}$ and $H = \text{PS}$ being produced in the q_1 and \bar{q}_1 splittings, can be performed as in Sec. IV A. The expression is similar to Eq. (36), with the third line substituted by the splitting function for VM emission $F_{q_2, h=\text{VM}, q_1}(M^2, Z_+, \mathbf{p}_T; \mathbf{k}_{1T}, C^{q_1 \bar{q}_1}) dM^2 Z_+^{-1} dZ_+ d^2 \mathbf{p}_T$. The expression for $F_{q_2, h=\text{VM}, q_1}$ is obtained by Eq. (21) taking $C_{x0}^{q_1 \bar{q}_1} = C_{y0}^{q_1 \bar{q}_1} = 0$. Instead, the splitting function $F_{\bar{q}_2, H, \bar{q}_1}(Z_-, \mathbf{P}_T; \bar{\mathbf{k}}_{1T}, C^{q_2 \bar{q}_1})$ can be obtained from Eq. (29). The latter depends on the correlation coefficients $C_{0x}^{q_2 \bar{q}_1}$ and $C_{0y}^{q_2 \bar{q}_1}$ for VM emission, which can be calculated using Eqs. (26) and (27). Assuming that the decay products of the VM are not analyzed, we obtain the correlation coefficients

$$\begin{aligned}
C_{0x}^{q_2 \bar{q}_1} &= C_{xx}^{q_1 \bar{q}_1} \frac{M_{x0}^{q_1}}{M_{00}^{q_1}} = + \frac{\sin^2 \theta}{1 + \cos^2 \theta} f_L \hat{a}(k_{2T}) (-\sin \phi_{k_2}^{q_1}), \\
C_{0y}^{q_2 \bar{q}_1} &= C_{yy}^{q_1 \bar{q}_1} \frac{M_{y0}^{q_1}}{M_{00}^{q_1}} = + \frac{\sin^2 \theta}{1 + \cos^2 \theta} f_L \hat{a}(k_{2T}) \cos \phi_{k_2}^{q_1}. \tag{39}
\end{aligned}$$

This leads to the probability distribution for $e^+e^- \rightarrow (h = \text{VM})(H = \text{PS})X$ [the analog of Eq. (38)]:

$$\begin{aligned}
\frac{dP(e^+e^- \rightarrow hHX)}{d \cos \theta dM^2 dZ_+ d^2 \mathbf{p}_T dZ_- d^2 \mathbf{P}_T} &\propto \frac{3}{8} (1 + \cos^2 \theta) \\
&\times \left(1 - \frac{\sin^2 \theta}{1 + \cos^2 \theta} f_L \hat{a}(p_T) \hat{a}(P_T) \cos(\phi_h^q + \phi_H^{\bar{q}}) \right). \tag{40}
\end{aligned}$$

Comparing with Eq. (38), one can see that the Collins asymmetry for back-to-back VM and PS mesons has the opposite sign with respect to the asymmetry for back-to-back PS mesons. Also, it is scaled by the factor f_L and it is thus sensitive to the fraction of longitudinally polarized VMs produced in hadronization. This is a genuine prediction of the string + 3P_0 model that could be tested experimentally, and it is similar to the prediction for the Collins asymmetries for VM production in SIDIS [27] and to the prediction for the single spin asymmetries for VM production in pp scattering [41].

The high precision BELLE [8] and BABAR [9] data could provide valuable information on the Collins asymmetry for, e.g., ρ^0 and π^\pm mesons produced back to back in e^+e^- annihilation. The measurement of such asymmetry would be useful to retrieve information on the free parameter f_L of the string + 3P_0 model for VM production. A negative asymmetry would be a confirmation of the prediction of the string + 3P_0 mechanism of hadronization.

V. CONCLUSIONS

We presented an extension of the string + 3P_0 model to the fragmentation of a string stretched between a quark q_1 and an antiquark \bar{q}_1 with entangled spin states. The spin correlations of the quarks are described by their joint spin-density matrix $\rho(q_1, \bar{q}_1)$. The latter is calculated assuming the quark pair to be produced in the annihilation of an electron and a positron via the exchange of a virtual photon and neglecting gluon radiation. The model is formulated as a recursive recipe that applies the rules of the string + 3P_0

model for the emission of hadrons from quark splittings as well as the Collins-Knowles recipe to take into account the spin correlations in the fragmentation chain. The recipe is general and it can be applied to other processes as well, regardless of the production mechanism of the $q_1\bar{q}_1$ pair.

To show that the proposed recipe reproduces the already predicted angular distribution of the final state hadrons, we carried a proof-of-concept calculation for the reaction $e^+e^- \rightarrow hHX$ where one of the hadrons is produced in the quark jet and the other in the antiquark jet. We obtained qualitatively the angular modulation in the distribution of the sum of the azimuthal angles of the two hadrons as expected by the product of two Collins effects. It agrees with the azimuthal correlation observed by the BELLE and BABAR experiments and predicts a reversal of the sign of the Collins asymmetry for back-to-back pseudoscalar and vector mesons.

For a deeper investigation of the model predictions a Monte Carlo implementation is required. The straightforward choice is the implementation in the PYTHIA generator by extending the StringSpinner package, which will be addressed in a separate work. Other improvements of the model are possible, such as the inclusion of gluon radiation. This development would be important to shed more light on the evolution of quark spin effects with the c.m.s. energy of the e^+e^- event.

ACKNOWLEDGMENTS

The authors are grateful to John Collins, Leif Lönnblad, and Anna Martin for the many useful discussions. The work of A. K. is done in the context of the project POLFRAG: Simulation of polarized quark fragmentation and application to the investigation of the nucleon structure, CUP No. J97G22000510001, funded by the Italian Ministry of University and Research (MUR).

APPENDIX A: HELICITY AMPLITUDES

The Feynman diagram associated to the process $e^+e^- \rightarrow q_1\bar{q}_1$, considering the exchange of one virtual photon, and its complex conjugate are shown in Fig. 9. We have indicated by λ_- , λ_+ , λ_1 , and $\bar{\lambda}_1$ the helicities of the e^- , e^+ , q_1 and \bar{q}_1 , respectively. The corresponding helicities in the complex conjugated diagram are λ'_- , λ'_+ , λ'_1 and $\bar{\lambda}'_1$. The helicity amplitude associated to the process $e^+e^- \rightarrow q_1\bar{q}_1$ is given by

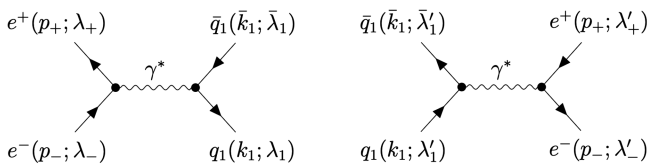


FIG. 9. Leading-order diagram for the process $e^+e^- \rightarrow q_1\bar{q}_1$ (left) and its complex conjugate (right). For each particle the momentum and helicity variables are shown in parentheses.

$$i\hat{\mathcal{M}}_{\lambda_-\lambda_+;\lambda_1\bar{\lambda}_1} = i\frac{4\pi\alpha}{s} [\bar{v}(e^+, \lambda_+)\gamma^\mu u(e^-, \lambda_-)] \times [\bar{u}(q_1, \lambda_1)\gamma_\mu v(\bar{q}_1, \bar{\lambda}_1)], \quad (\text{A1})$$

where u and v indicate the Dirac spinors in the helicity basis for a fermion and an antifermion, respectively.

The explicit expressions of $\hat{\mathcal{M}}_{\lambda_-\lambda_+;\lambda_1\bar{\lambda}_1}$ have been calculated keeping the quark mass m_q , and the results are shown in Table I for the different combinations of the helicity pairs (λ_-, λ_+) and $(\lambda_1, \bar{\lambda}_1)$. If the quark masses are neglected, there are only two pairs of nonvanishing matrix elements, i.e. $\hat{\mathcal{M}}_{-+;-+} = \hat{\mathcal{M}}_{-+;+-}$ and $\hat{\mathcal{M}}_{+-;-+} = \hat{\mathcal{M}}_{+-;+-}$ (the equalities hold because of parity conservation).

If the quark mass is taken into account, the two other pairs of matrix elements $\hat{\mathcal{M}}_{-+;+-} = \hat{\mathcal{M}}_{-+;--}$ and $\hat{\mathcal{M}}_{+-;+-} = \hat{\mathcal{M}}_{+-;--}$ show up. They involve helicity nonconservation at the quark creation vertex. The explicit expressions are shown in Table I. These matrix elements are suppressed by the Lorentz factor $\gamma_q = 1/\sqrt{1-\beta_q^2}$. For charmed quarks, it is $\gamma_c \simeq 3.57$ in the kinematics of the BELLE and BABAR experiments and $\gamma_c \simeq 1.20$ and in the kinematics of the BESIII experiment.

APPENDIX B: SPIN PROPAGATION AFTER A HADRON EMISSION FROM THE \bar{q}_1 END

We consider here the case of a hadron H that is emitted in the splitting $\bar{q}_1 \rightarrow H + \bar{q}_2$ taken from the antiquark end of a string stretched between the quark q_2 and the antiquark \bar{q}_1 . The joint spin-density matrix of the $q_2\bar{q}_1$ system is described by the correlation coefficients $C^{q_2\bar{q}_1}$, calculated using Eq. (26).

1. Density matrix and decay of the VM

If $H = \text{VM}$, its spin-density matrix can be most simply calculated using Eq. (22) with the replacement $T_{q_2,h=\text{VM},q_1}^a \otimes 1^{\bar{q}_1} \rightarrow 1^{q_1} \otimes T_{\bar{q}_2,H=\text{VM},\bar{q}_1}^a$ and $T_{q_2,h=\text{VM},q_1}^{\dagger a'} \otimes 1^{\bar{q}_1} \rightarrow 1^{q_1} \otimes T_{\bar{q}_2,H=\text{VM},\bar{q}_1}^{\dagger a'}$. Using the expression for the splitting amplitude in Eq. (15), the spin-density matrix is

$$\rho_{aa'}(H) = \frac{C_{0\beta}^{q_2\bar{q}_1} \text{Tr}[\Delta(\bar{\mathbf{k}}_{2T})\Gamma_a(H)\sigma_\beta^{\bar{q}_1}\Gamma_{a'}^\dagger(H)\Delta^\dagger(\bar{\mathbf{k}}_{2T})]}{\text{Tr}[\dots]}. \quad (\text{B1})$$

The spin-density matrix is used to generate the decay of H , as described in Sec. III A 2. In this case, however, the polar and azimuthal angles involved in the distribution of the decay hadrons [see Eq. (24)] are defined in the AHF. They can be expressed in the QHF by using Eq. (9).

2. Calculation of the new correlation coefficients

After the emission of H (and after its decay, if it is a VM), a new string piece stretched between q_2 and \bar{q}_2 remains. The joint spin-density matrix of the $q_2\bar{q}_2$ system

can be calculated as in Eq. (25) using the replacement $T_{q_2, h=PS, q_1} \otimes 1^{\bar{q}_1} \rightarrow 1^{q_1} \otimes T_{\bar{q}_2, H=PS, \bar{q}_1}$ if $H = PS$ and the replacement $T_{q_2, h=VM, q_1} \otimes 1^{\bar{q}_1} \rightarrow 1^{q_1} \otimes T_{\bar{q}_2, H=VM, \bar{q}_1}^a$ if $H = VM$. The new joint spin-density matrix is thus given by

$$\rho(q_2, \bar{q}_2) = \begin{cases} \mathbf{T}_{\bar{q}_2, H, \bar{q}_1} \rho(q_2, \bar{q}_1) \mathbf{T}_{\bar{q}_2, H, \bar{q}_1}^\dagger / \text{Tr}[\dots] & H = PS, \\ \mathbf{T}_{\bar{q}_2, H, \bar{q}_1}^a \rho(q_2, \bar{q}_1) \mathbf{T}_{\bar{q}_2, H, \bar{q}_1}^{\dagger a'} D_{a'a} / \text{Tr}[\dots] & H = VM. \end{cases} \quad (\text{B2})$$

The correlation coefficients for the $q_2 \bar{q}_2$ system can be calculated using Eq. (B2) and the explicit expression for the splitting amplitude in Eq. (15). They are

$$C_{\alpha\beta'}^{q_2 \bar{q}_2} = C_{\alpha\beta}^{q_1 \bar{q}_1} M_{\beta\beta'}^{\bar{q}_1} / C_{0\beta}^{q_1 \bar{q}_1} M_{\beta 0}^{\bar{q}_1}, \quad (\text{B3})$$

where the matrix $M_{\beta\beta'}^{\bar{q}_1}$ is given by

$$M_{\beta\beta'}^{\bar{q}_1}|_{PS} = \frac{1}{2} \text{Tr}[\sigma_{\beta'}^{\bar{q}_1} \Delta(\bar{\mathbf{k}}_{2T}) \Gamma_H \sigma_{\beta}^{\bar{q}_1} \Gamma_H^\dagger \Delta^\dagger(\bar{\mathbf{k}}_{2T})] \\ M_{\beta\beta'}^{\bar{q}_1}|_{VM} = \frac{1}{2} \text{Tr}[\sigma_{\beta'}^{\bar{q}_1} \Delta(\bar{\mathbf{k}}_{2T}) \Gamma^a(H) \sigma_{\beta}^{\bar{q}_1} \Gamma^{\dagger a'}(H) \Delta^\dagger(\bar{\mathbf{k}}_{2T})] D_{a'a}. \quad (\text{B4})$$

Equations (B3) and (B4) are, respectively, the analogs of Eqs. (26) and (27) that apply when the meson is emitted from the quark side. The matrix $M_{\alpha\beta}^{\bar{q}_1}$ in Eq. (B4) can be obtained from Eq. (27) by the substitutions $q_1 \rightarrow \bar{q}_1$, $h \rightarrow H$ and $\mathbf{k}_{2T} \rightarrow \bar{\mathbf{k}}_{2T}$. The matrix $D_{aa'}$ is the decay matrix of H , which is calculated as in Sec. III A 2.

APPENDIX C: STEPS FOR THE SIMULATION OF THE ANTIQUARK SPLITTING

The steps for the simulation of the antiquark splitting are similar to those for the quark splitting described in points 2 and 3 in Sec. III B. They are the following.

- (a) Select a new quark pair $q_2 \bar{q}_2$ with probability $\hat{u}_{\bar{q}_1, H} / \hat{u}_{\bar{q}_1}$ using Eq. (14). Form the hadron $H = (\bar{q}_1 q_2)$ and decide whether it is a VM with probability f_{VM} , or a PS meson. If H is a PS meson, generate $\bar{\mathbf{k}}_{2T}^2$, $\phi_{\bar{\mathbf{k}}_2}^{\bar{q}_1}$ and Z_- using the splitting function $F_{\bar{q}_2, H=PS, \bar{q}_1}(Z_-, \mathbf{P}_T; \bar{\mathbf{k}}_{1T}, C^{q_2 \bar{q}_1})$ in Eq. (29). If H is a VM, use instead the splitting function $F_{\bar{q}_2, H=VM, \bar{q}_1}(M^2, Z_-, \mathbf{P}_T; \bar{\mathbf{k}}_{1T}, C^{q_2 \bar{q}_1})$ in Eq. (30) to generate first the invariant mass squared M^2 and then $\bar{\mathbf{k}}_{2T}^2$, $\phi_{\bar{\mathbf{k}}_2}^{\bar{q}_1}$ and Z_- . Calculate the light-cone momenta $P^- = Z_- \bar{k}_1^-$ and $P^+ = \varepsilon_H^2 / P^-$ and construct the four-momentum of H using $P = (E_H, \mathbf{P}_T, P_L)$, where $E_H = (P^+ + P^-)/2$ and $P_L = (P^+ - P^-)/2$. Express P in the QHF using Eq. (9). Before accepting the generated P , update the new available light-cone momenta $(P_{\text{tot}}^-)^{\text{new}} = P_{\text{tot}}^- - P^-$ and $(P_{\text{tot}}^+)^{\text{new}} = P_{\text{tot}}^+ - \varepsilon_H^2 / P^-$ and the transverse momentum $\mathbf{P}_{\text{tot}, T}^{\text{new}} = \mathbf{P}_{\text{tot}, T} - \mathbf{P}_T$. If $P_{\text{tot}}^2 < M_{\text{min}}^2$, go to step 4 in Sec. III B. Otherwise define $P_{\text{tot}} = P_{\text{tot}}^{\text{new}}$.
 - (a.1) Calculate the spin-density matrix of H using Eq. (B1) and generate the momenta of the decay hadrons in the rest frame of H using Eq. (23). Express the momenta in the QHF using Eq. (9). The expressions for the decay amplitude \mathcal{M} can be found in Ref. [27].
 - (a.2) Calculate the decay matrix D using Eq. (24).
 - (a.3) To come back to the center of mass frame, apply the composition of longitudinal and transverse boosts in Ref. [27] to the decay hadrons.
- (b) Calculate the correlation coefficients $C^{q_2 \bar{q}_2}$ of the new string piece with end points q_2 and \bar{q}_2 using Eqs. (B3) and (B4). Let \bar{q}_2 , \bar{k}_2 and $C^{q_2 \bar{q}_2}$ take the place of \bar{q}_1 , \bar{k}_1 and $C^{q_1 \bar{q}_1}$ and then go to step 1 in Sec. III B.

[1] J. C. Collins and D. E. Soper, Back-to-back jets in QCD, *Nucl. Phys.* **B193**, 381 (1981); **B213**, 545(E) (1983).
 [2] J. C. Collins, Fragmentation of transversely polarized quarks probed in transverse momentum distributions, *Nucl. Phys.* **B396**, 161 (1993).
 [3] J. C. Collins, S. F. Heppelmann, and G. A. Ladinsky, Measuring transversity densities in singly polarized hadron hadron and lepton—hadron collisions, *Nucl. Phys.* **B420**, 565 (1994).
 [4] A. Bianconi, S. Boffi, R. Jakob, and M. Radici, Two hadron interference fragmentation functions. Part 1. General framework, *Phys. Rev. D* **62**, 034008 (2000).

[5] D. Boer, Angular dependences in inclusive two-hadron production at BELLE, *Nucl. Phys.* **B806**, 23 (2009).
 [6] X. Artru and J. C. Collins, Measuring transverse spin correlations by 4 particle correlations in $e^+e^- \rightarrow 2$ jets, *Z. Phys. C* **69**, 277 (1996).
 [7] R. Seidl *et al.* (Belle Collaboration), Measurement of azimuthal asymmetries in inclusive production of hadron pairs in e^+e^- annihilation at $\sqrt{s} = 10.58$ -GeV, *Phys. Rev. D* **78**, 032011 (2008); **86**, 039905(E) (2012).
 [8] H. Li *et al.* (Belle Collaboration), Azimuthal asymmetries of back-to-back $\pi^\pm - (\pi^0, \eta, \pi^\pm)$ pairs in e^+e^- annihilation, *Phys. Rev. D* **100**, 092008 (2019).

- [9] J. P. Lees *et al.* (BABAR Collaboration), Measurement of Collins asymmetries in inclusive production of charged pion pairs in e^+e^- annihilation at BABAR, *Phys. Rev. D* **90**, 052003 (2014).
- [10] J. P. Lees *et al.* (BABAR Collaboration), Collins asymmetries in inclusive charged KK and $K\pi$ pairs produced in e^+e^- annihilation, *Phys. Rev. D* **92**, 111101 (2015).
- [11] M. Ablikim *et al.* (BESIII Collaboration), Measurement of azimuthal asymmetries in inclusive charged dipion production in e^+e^- annihilations at $\sqrt{s} = 3.65$ GeV, *Phys. Rev. Lett.* **116**, 042001 (2016).
- [12] A. Vossen *et al.* (Belle Collaboration), Observation of transverse polarization asymmetries of charged pion pairs in e^+e^- annihilation near $\sqrt{s} = 10.58$ GeV, *Phys. Rev. Lett.* **107**, 072004 (2011).
- [13] M. Anselmino, M. Boglione, U. D'Alesio, S. Melis, F. Murgia, and A. Prokudin, Simultaneous extraction of transversity and Collins functions from new SIDIS and e^+e^- data, *Phys. Rev. D* **87**, 094019 (2013).
- [14] M. Anselmino, M. Boglione, U. D'Alesio, J. O. Gonzalez Hernandez, S. Melis, F. Murgia, and A. Prokudin, Collins functions for pions from SIDIS and new e^+e^- data: A first glance at their transverse momentum dependence, *Phys. Rev. D* **92**, 114023 (2015).
- [15] A. Martin, F. Bradamante, and V. Barone, Extracting the transversity distributions from single-hadron and dihadron production, *Phys. Rev. D* **91**, 014034 (2015).
- [16] M. Anselmino, M. Boglione, U. D'Alesio, J. O. Gonzalez Hernandez, S. Melis, F. Murgia, and A. Prokudin, Extracting the Kaon Collins function from e^+e^- hadron pair production data, *Phys. Rev. D* **93**, 034025 (2016).
- [17] Z.-B. Kang, A. Prokudin, P. Sun, and F. Yuan, Extraction of quark transversity distribution and Collins fragmentation functions with QCD evolution, *Phys. Rev. D* **93**, 014009 (2016).
- [18] J. Cammarota, L. Gamberg, Z.-B. Kang, J. A. Miller, D. Pitonyak, A. Prokudin, T. C. Rogers, and N. Sato (Jefferson Lab Angular Momentum Collaboration), Origin of single transverse-spin asymmetries in high-energy collisions, *Phys. Rev. D* **102**, 054002 (2020).
- [19] M. Radici, A. Courtoy, A. Bacchetta, and M. Guagnelli, Improved extraction of valence transversity distributions from inclusive dihadron production, *J. High Energy Phys.* **05** (2015) 123.
- [20] C. Cocuzza, A. Metz, D. Pitonyak, A. Prokudin, N. Sato, and R. Seidl, Transversity distributions and tensor charges of the nucleon: Extraction from dihadron production and their universal nature, *Phys. Rev. Lett.* **132**, 091901 (2024).
- [21] T. Sjostrand, S. Mrenna, and P. Z. Skands, A brief introduction to PYTHIA 8.1, *Comput. Phys. Commun.* **178**, 852 (2008).
- [22] C. Bierlich *et al.*, A comprehensive guide to the physics and usage of PYTHIA 8.3, *SciPost Phys. Codebases* **8** (2022), 10.21468/SciPostPhysCodeb.8.
- [23] A. Kerbizi and L. Lönnblad, StringSpinner—adding spin to the PYTHIA string fragmentation, *Comput. Phys. Commun.* **272**, 108234 (2022).
- [24] A. Kerbizi and L. Lönnblad, Extending StringSpinner to handle vector-meson spin, *Comput. Phys. Commun.* **292**, 108886 (2023).
- [25] A. Kerbizi, X. Artru, Z. Belghobsi, F. Bradamante, and A. Martin, Recursive model for the fragmentation of polarized quarks, *Phys. Rev. D* **97**, 074010 (2018).
- [26] A. Kerbizi, X. Artru, Z. Belghobsi, and A. Martin, Simplified recursive 3P_0 model for the fragmentation of polarized quarks, *Phys. Rev. D* **100**, 014003 (2019).
- [27] A. Kerbizi, X. Artru, and A. Martin, Production of vector mesons in the string + 3P_0 model of polarized quark fragmentation, *Phys. Rev. D* **104**, 114038 (2021).
- [28] B. Andersson, G. Gustafson, G. Ingelman, and T. Sjostrand, Parton fragmentation and string dynamics, *Phys. Rep.* **97**, 31 (1983).
- [29] K. Chen, G. R. Goldstein, R. L. Jaffe, and X.-D. Ji, Probing quark fragmentation functions for spin 1/2 baryon production in unpolarized e^+e^- annihilation, *Nucl. Phys.* **B445**, 380 (1995).
- [30] J. C. Collins, Spin correlations in Monte Carlo event generators, *Nucl. Phys.* **B304**, 794 (1988).
- [31] I. G. Knowles, Spin correlations in parton—parton scattering, *Nucl. Phys.* **B310**, 571 (1988).
- [32] P. Richardson, Spin correlations in Monte Carlo simulations, *J. High Energy Phys.* **11** (2001) 029.
- [33] U. D'Alesio, F. Murgia, and M. Zaccarddu, General helicity formalism for two-hadron production in e^+e^- annihilation within a TMD approach, *J. High Energy Phys.* **10** (2021) 078.
- [34] X. Artru, M. Elchikh, J.-M. Richard, J. Soffer, and O. V. Teryaev, Spin observables and spin structure functions: Inequalities and dynamics, *Phys. Rep.* **470**, 1 (2009).
- [35] P. Abreu *et al.* (DELPHI Collaboration), Measurement of the spin density matrix for the ρ^0 , $K^{*0}(892)$ and F produced in Z^0 decays, *Phys. Lett. B* **406**, 271 (1997).
- [36] G. Abbiendi *et al.* (OPAL Collaboration), A study of spin alignment of $\rho(770)^\pm$ and $\omega(782)$ mesons in hadronic Z^0 decays, *Eur. Phys. J. C* **16**, 61 (2000).
- [37] A. Anselm, M. Anselmino, F. Murgia, and M. G. Ryskin, On the parton interpretation of quark fragmentation into hadrons with different spins, *JETP Lett.* **60**, 496 (1994).
- [38] M. Boglione and A. Simonelli, Full treatment of the thrust distribution in single inclusive $e^+e^- \rightarrow hX$ processes, *J. High Energy Phys.* **09** (2023) 006.
- [39] R. L. Workman *et al.* (Particle Data Group), Review of particle physics, *Prog. Theor. Exp. Phys.* **2022**, 083C01 (2022).
- [40] E. Leader, *Spin in Particle Physics* (Cambridge University Press, Cambridge, England, 2011), Vol. 15.
- [41] J. Czyzewski, Single spin asymmetry of vector meson production in the string model, *Acta Phys. Pol. B* **27**, 1759 (1996).